İSTANBUL TECHNICAL UNIVERSITY ★ INSTITUTE OF SCIENCE AND TECHNOLOGY

DESIGN AND THE APPLICATION OF A CAPILLARY RHEOMETER TO THE DETERMINATION OF THE FLOW CHARACTERISTICS OF HDPE

M.Sc. Thesis by
İsminur GÖKGÖZ

Department: **Polymer Science and Technology**

Programme: **Polymer Science and Technology**

JANUARY 2008

İSTANBUL TECHNICAL UNIVERSITY ★ INSTITUTE OF SCIENCE AND TECHNOLOGY

DESIGN AND THE APPLICATION OF A CAPILLARY RHEOMETER TO THE DETERMINATION OF THE FLOW CHARACTERISTICS OF HDPE

M.Sc. Thesis by

İsminur GÖKGÖZ

(515041022)

Date of submission : 24 December 2007

Date of defence examination: 28 January 2008

Supervisor (Chairman): **Prof. Dr. F. Seniha GÜNER**

Members of the Examining Committee **Prof.Dr. Nurseli UYANIK (İ.T.Ü.)**

Prof.Dr. İsmail TEKE (Y.T.Ü.)

JANUARY 2008

İSTANBUL TEKNİK ÜNİVERSİTESİ ★ FEN BİLİMLERİ ENSTİTÜSÜ

HDPE'NİN AKIŞ KARAKTERİSTİKLERİNİN BELİRLENMESİ İÇİN BİR KAPİLER REOMETRE TASARIMI VE UYGULANMASI

YÜKSEK LİSANS TEZİ
İsminur GÖKGÖZ
(515041022)

Tezin Enstitüye Verildiği Tarih : 24 Aralık 2007
Tezin Savunulduğu Tarih : 28 Ocak 2008

Tez Danışmanı :	**Prof.Dr. F.Seniha GÜNER**
Diğer Jüri Üyeleri	**Prof.Dr. Nurseli UYANIK (İ.T.Ü.)**
	Prof.Dr. İsmail TEKE (Y.T.Ü.)

OCAK 2008

PREFACE

Firstly, I would like to thank my adviser, Prof. Dr. Seniha Güner, Prof. Dr. Nurseli Uyanık and Dizayn Group Reseach and Technology Development department for their invaluable supports. Especially, I would like to thank Dr. Zafer Gemici, department manager, for always being there to encourage me and help in guiding me on some mechanical engineering problems with Prof. Dr. İsmail Teke. I would like to thank appreciate the support offered by my friends, Süleyman Deveci, Ümit Güler, Oktay Yılmaz, Volkan Uçar and especially Tamer Birtane for help in technical drawing of rheometer. I would like also to thank Atomika Technic Company which is distributor of Malvern Instrument, Yrd. Doç. Dr. Necati Özkan and Dr.İlhan Özen for their advices. Lastly, I would like to thank my parents for their continued supports.

January 2008 İsminur GÖKGÖZ

TABLE OF CONTENTS

ABBREVIATIONS

ASTM	**:** American Society for Testing and Materials
EPDM	**:** Ethylene/propylene/diene rubber
HDPE	**:** High density polyethylene
LDPE	**:** Low density polyethlene
LLDPE	**:** Lineer low density polyethylene
MCPE	**:** Metallocene catalyzed polyethylene
MFI	**:** Melt flow index
MFR	**:** Melt flow rate
MDPE	**:** Medium density polyethylene
PE	**:** Polyethylene
PEEK	**:** Polyetheretherketone
PES	**:** Polyether sulfone
PMMA	**:** Polymethyl methacrylate
PP	**:** Polypropylene
UHDPE	**:** Ultra high density polyethylene

LIST of TABLES

Page No

LIST of FIGURES

Page No

LIST of SYMBOLS

a	: Carreau-Yasuda index
a_T	: Shifting factor
A	: Area
c_p	: Specific heat
C_1', C_2'	: WLF equation constants
h	: Distance
D_p	: Extrudate diameter
D_c	: Capillary diameter
D_b	: Barrel diameter
D_{piston}	: Piston diameter
ΔE	: Activation energy
F	: Force
H	: Gap between the two parallel discs
k	: Consistency index
I	: Moment
L	: Lenght of die
L_a	: Actual length of the column
L_e	: Effective length
L_p	: Lenght of the piston
m_{barrel}	: Mass of the barrel
m	: Cross law index
$\bar{M}_w$	: Weight average molecular weight
$\bar{M}_c$	: Critical molecular weight
n	: Power law exponent
N	: Design factor
Na	: Nahme number
N_1	: First normal stress difference
N_2	: Second normal stress difference
N_3	: Third normal stress difference
P	: Pressure
p	: Hydrostatic pressure
Q	: Volumetric flow rate
Q_{total}	: Total volumetric flow rate
r	: Radius of gyration
R	: Universal gas constant
R	: Die radius

R_d : Radius of the disc

R_b : Barrel radius

R_0 : Radius of outer cylinder

R_i : Radius of inner cylinder

R_p : Radius of the plate

R_w : Radius of the roller

S : Wall thickness

S_y : Yield strenght

t : Time

T : Torque

T : Temperature

T_0 : Referance temperature

T_g : Glass transition temperature

T_s : Standart temperature

ν : Angular velocity

ν_s : Wall slip velocity

V : Velocity

V_R : Velocity at coaxial rheometry

V_{barrel} : Volume of barrel

V_p : Piston speed

V_s : Slip velocity

ΔPc : Pressure drop across the capillary

ΔP_{ent} : Entrance pressure drop

ΔP_{total} : Total pressure drop

ΔT : Temperature difference

γ : Shear strain

$\dot{\gamma}$: Shear rate

α : Cone angle

β : Pressure coefficient

η : Shear viscosity

η_{ap} : Apparent shear viscosity

η_0 : Zero shear viscosity

η_∞ : Infinity shear viscosity

Ω : Rotational speed

μ : Density

τ : Shear stress at the capillary wall

σ : Tensile strength value of barrel material

τ_c : Critical wall shear stress

τ_e : Extensional stress

ω : Angular velocity

HDPE'NİN AKIŞ KARAKTERİSTİKLERİNİN BELİRLENMESİ İÇİN BİR KAPİLER REOMETRE TASARIMI VE UYGULANMASI

ÖZET

Plastik malzemelerin üretim prosesini anlayabilmek için, kullanılan ekipman özelliklerini bilmek yeterli değil aynı zamanda malzeme davranışlarının da bilinmesi gerekir.

Bu durumda, reoloji malzemelerin proses koşulları altındaki akış davranışlarının tespitinde önemli bir rol oynar. Bilindiği gibi reoloji malzemelerin uygulanan bir gerilim altındaki akış ve deformasyonu ile ilgilenir.

Günümüzde, malzemelerin reolojik özelliklerini karakterize etmek için kullanılan bir çok çeşitte reometreler vardır. Bunlar rotasyonel ve kapiler reometre olmak üzere iki geniş katagoriye ayrılabilirler. Rotasyonel reometreler genellikle malzemelerin düşük kayma oranlarındaki akış özelliklerini belirlemek için tercih edilirler. Aynı zamanda malzemelerin elastik özelliklerini tespit etmek için de kullanılabilirler. Bunun dışında bir kapiler reometre malzemelerin daha yüksek kayma oranlarındaki akış özelliklerini belirlemek için tercih edilirler.

Kapiler reometrenin kayma oranı kontrollü, nitrojen gazlı, iki ya da üç hazneli gibi. bir çok çeşidi vardır. Bu çalışmada, malzemelerin akış özelliklerini tespit edebilmek için kayma oranı kontrollü kapiler reometre dizayn edildi. Test cihazı bir hazne, bir piston, ısıtma ve sıcaklık kontrol aygıtları, bir basınç sensörü ve bir kalıptan oluşmakta. İhtiyaç duyulan sabit piston hızı bir basma-çekme test cihazından sağlanmış ve kalıp boyunca oluşan basınç düşmesini hesaplamak için kalıp girişine bir basınç sensörü yerleştirilmiştir. Montaj işlemi tamamlandıktan sonra, yüksek yoğunluklu polietilenin akış davranışları bu kapiler reometre ile test edilmiştir.

Bu çalışmada, kayma gerilmesi değerlerinin hesabı için Bagley Düzeltmesi'ne göre aynı çapta ve farklı uzunluklarda dört adet kalıp kullanılmıştır. Rabinowitch Düzetmesi ve Güç Yasası da kayma oranı ve kayma viskozitesini hesaplamak için kullanılmıştır. Sonuçları kıyaslamak için, yüksek yoğunluklu polietilen diğer ticari kapiler reometreler ile test edilmiştir.

DESIGN AND THE APPLICATION OF A CAPILLARY RHEOMETER TO THE DETERMINATION OF THE FLOW CHARACTERISTICS OF HDPE

SUMMARY

In order to understand a process for the production of plastic material, it is not enough to know the properties of equipment used but the material behavior should be known.

In this case, rheology plays an important role in understanding of flow behavior of materials under the processing conditions. It is well-known that, rheology is concerned with the flow and deformation of materials under an applied stress.

Nowadays, there are various types of rheometers used to characterize the rheological properties of materials. They can be divided into two broad categories, rotational and capillary rheometer. Rotational rheometers are generally preferred to determine flow properties of materials at low shear rates. At the same time, they can also used for determination of elastic properties of materials. Except from this, a capillary rheometer is generally preferred to determine flow behavior of materials at higher shear rates.

There are various types of capillary rheometer such as controlled shear rate, nitrogen driven, twin or trible bore. In this study, a capillary rheometer with controlled shear rate was designed to determine flow properties of polymers. Test apparatus consists of a barrel, a piston, heating and temperature control devices, a pressure transducer and a die. Required constant piston speed was generated by tensile testing machine and a pressure transducer was mounted just above the capillary die to record the pressure drop along the die. After the assembling, the flow behaviour of high density polyethylene was determined by this capillary rheometer.

In this study, four dies which have same diameter and different lengths were used to determine shear stress values according to the Bagley Correction. Rabinowitch Correction and Power Law were also used to determine shear rate and shear viscosity values, respectively. In order to compare the resuts, high density polyethylene was tested with other commercial capillary rheometers.

1. INTRODUCTION

Nowadays, polymers are processed via extrusion, injection or blown molding etc. Depending on the usage area and the type of the polymers most of the process contains melting and extrusion steps. At that point we need rhoelogical data for determination of polymer behavior

Rheology is the science of the deformation and flow of materials, and based on the laws of elasticity and viscosity. The science of rheology is young but its history is very old. In the 17th century, the basic laws of elasticity and simple viscous flow were carried out by Robert Hooke and Isaac Newton, respectively. In 1839, the first recorded study of the viscosity of a liquid has been done by Hagen. He found that the pressure drop for capillary flow depended on viscosity and kinetic energy. In 1841, Poiseuille studied on flow in capillary and found that flow rate was proportional to the pressure gradient. Pionerring work on the laws of motion for fluids was formulated by Navier and Stokes. Hence, some important equations could be solved.

In 1929, rheology was introduced as a formal scientific discipline at Third Plasticity Symposium and The Society of Rheology was officially formed on Dec. 9, 1929. The Greek letters on the hourglass logo of The Society of Rheology, παντα ρει, (sometimes pronounced phonetically “panta rei”) may be translated “everything flows”. This phrase is attributed to the Greek philosopher Heraclitus of Ephesus [1].

Developments in rheology related to the post-inception period are shown in Table 1.1[2].

Table 1.1: Rheology since its inception in 1929.

Area of Activity		Representative Works
Constitutive equations	a) Differential models	Oldroyd (1950), Truesdell (1952), Rivlin & Ericsen (1955), Giesekus (1962), White-Metzner (1963)
	b) Integral models	Green & Rilvin (1957), Coleman & Noll (1961)
	c) Network models	Green & Tobolsky (1946), Lodge (1956), Yamamoto (1956)
	d) Reptation models	Edwards (1967), De Gennes (1971), Doi & Edwards (1978)
	e) Molecular models	Kuhn (1934), Rouse (1953), Zimm (1956), Bird et al. (1987)
Experimental advances and rheological descriptions	a) Shear flows and the no-slip boundary condition	Money (1931,1936), Schofield & Blair (1930), Pearson & Petrie (1968), Ramamurthy (1986)
	b) Normal stresses and rod-climbing effects	Lander (1945), Weissenberg (1947), Markowitz (1957), Ginn & Metzner (1969)
	c) Dynamic studies	Eisenschitz & Philippoff (1933), Leaderman (1943), Cox-Merz (1958)
	d) Thixotropy	Freundlich & Bircumshaw (1926), Cheng & Evans (1965), Mewis (1979), Barnes (1997)
	e) Flow instabilities	Nason (1945), Tordella (1958), Petrie & Denn (1976)
	f) Extensional behaviour	Merrington (1943), Ballman (1965), Cogswell (1969), Metzner (1968), Dealy at al. (1976), Laun & Munstedt (1978)
Computational rheology	a) Continuum simulations	Turner at al. (1956), Cruse & Risso (1968), Beris et al. (1987), Walters & Taner (1992)
	b) Molecular dynamic simulations	Adler & Wainright (1957), Ashurst & Hoover (1975), Davis & Todd (1998)

Many different instruments called rheometer are used for determination of flow behavior of materials. They are divided into two broad categories, rotational and capillary rheometer. Rotational rheometers are capable of many tests to determine of material flow properties over a range temperatures and flow rates. For example, flow curves are determined at sufficiently low shear rates and hence zero shear viscosity value can be measure to know how viscosity change with average molecular weight of polymer. Relaxation and creep tests can also be apply to determine the amount of elasticity in the sample. The main difference between rotational and capillary rheometer is that, capillary rheometer can determine shear and extensional viscosities of a polymer melts. Die swell or extrudate strength can be also measured using additional accessories. Generally, capillary rheometers are used to measure melt properties at under typical processing conditions such as extrusion.

Driving force instrument and dies are very expensive apparatus used in capillary rheometers. The price of a die chances with entry angle, length/diameter ratio (L/D) or die's material. A Celsum's die, for example, costs 400-600£. Pressure transducer and additional apparatus such as laser micrometer and rheotens can also increase the price of rheometer. Hence, capillary rheometer is not as cheap as a melt flow index.

In this study, a capillary rheometer was designed. Required piston movement was provided by a tensile testing machine and dies weren't bought from a capillary rheometer producer. All dies were produced in Turkey. In the first step of the study, suitable die material was selected and many tests were done to provide desired surface finishing value. Then, suitable die, piston and barrel sizes were determined. After designing the rheometer, it was establish in the laboratory and tested for high density polyethylene (HDPE).

2. BASIC CONCEPTS of POLYMER MELT RHEOLOGY

One way of characterising a material is by its relaxation time, the time required to reduce a stress in the material by flow. Another way of defining materials rheologically is by the terms viscous, elastic or viscoelastic.

One of the main issues of rheology is the definition and classification of materials. Normal glass, for instance, is usually defined as a solid material, but if the thickness of an old church window is measured from top to bottom a difference will be noted. Glass does in fact flow like a liquid, albeit very slowly [3].

2.1. Shear Viscosity

The term viscosity, or resistance to flow is subdivided into two category, shear and elongation viscosity. As the name suggest, shear viscosity is resistance to shearing flow, and elongational viscosity is the resistance to elongation. Since the shear deformation occurs when a polymer flows in a capillar, shear viscosity is discussed in detail below.

The most important difference between the Newtonian and non-Newtonian flow is shear viscosity. Because Newtonian fluid has constant viscosity value at all shear rates but non-Newtonian fluid hasn't. When a Newtonian fluid is placed between the two plates and a force is applied to the top surface, a deformation occurs as seen in Figure 2.1.[4].

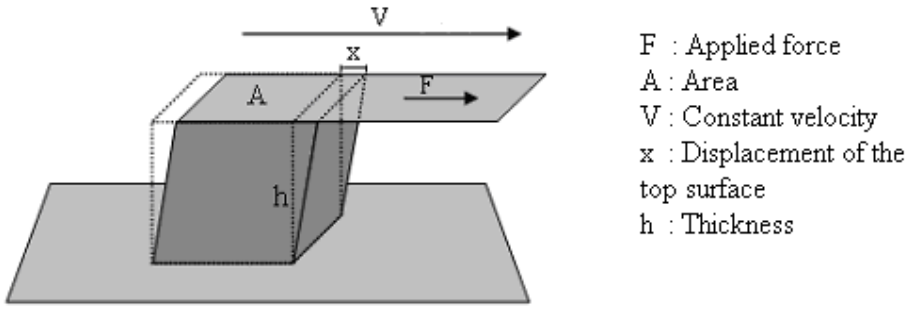

Figure 2.1: Simple shear deformation.

The amount of this deformation is measured by the shear strain Equation 2.1.

$$\gamma = \frac{x}{h} \tag{2.1}$$

Shear strain is dimensionless and is usually called as a percentage. Shear rate is known as the rate of change of shear strain by the time (t) calculated by Equation 2.2. Shear stress can be calculated from Equation 2.3.

$$\dot{\gamma} = \frac{d\gamma}{dt} = \frac{V}{h} \tag{2.2}$$

$$\tau = \frac{F}{A} \tag{2.3}$$

In this way, shear viscosity can be find mathematically by Equation 2.4.

$$\eta = \frac{\tau}{\dot{\gamma}} \tag{2.4}$$

Here η is called the Newtonian viscosity.

Although viscosity of many fluids, such as water or low molecular weight liquids, is well characterized by Newton's law, other fluids, such as polymer solution and melts, blood, mayonnaise, toothpaste and ink, are not characterized well by Newton's law. These fluids are called non-Newtonian fluids.

2.1.1. Various types of Fluids

Many fluids can react in different ways under the same conditions. For example, the viscosity of many fluids decreases with increasing shear rate while some fluid's don't as seen in Figure 2.2.[4]. According to their flow behavior, fluids can be classifed as Newtonian, Pseudoplastic (Shear Thinning), Dilatant, Bingham, Thixotropic or Rheopectic.

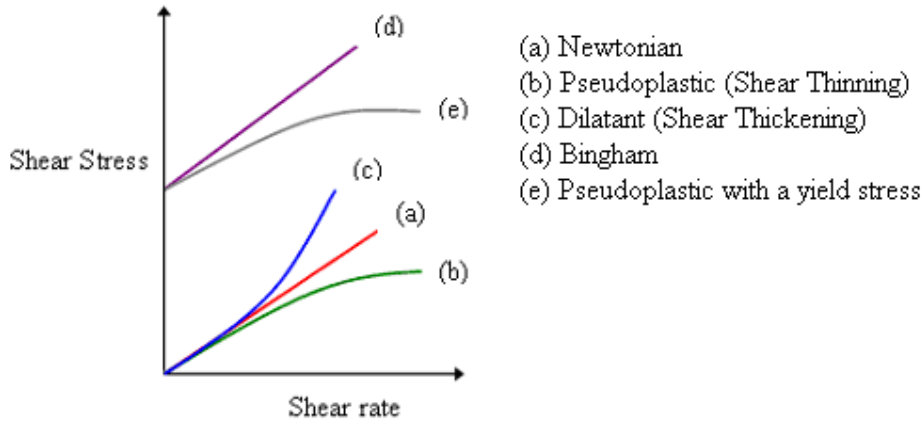

Figure 2.2: Flow curves of fluids without a yield stress and with a yield stress.

Fluids can be classifed according to the their flow curve.

Newtonian Fluid: As mentioned before, viscosity of this fluid doesn't change with increasing shear rate.

Pseudoplastic (Shear Thinning): The viscosity of a shear thinning fluid, sometimes also named pseudoplastic, decreases with increasing shear rate. As known the plastic molecules consist of long and entangled molecules and the viscosity of a polymer is determined by these entanglements. When a polymer is exposed to a high shear rate, entanglements of the polymer molecules reduces then viscosity reduces. When the shear rate is reduced, the viscosity increases again. Typical examples of shear thinning fluids are cream, shampoo, polymer mets and solutions.

Dilatant (Shear Thickening): These fluids show an increase in viscosity with increasing shear rate. This type of flow behaviour is generally found among suspensions of very high concentration. The solvent acts as a lubricant between suspended particles at low shear rates but is squeezed out at higher shear rates, resulting in denser packing of the particles. Typical examples of shear thickening systems are wet sand and concentrated starch suspensions.

Bingham plastics: Bingham fluids have a yield stress and do not flow unless the stress applied exceeds a certain minimum value of yield stress. Below this yield stress the fluid will behave almost like a solid and above as a liquide. Examples of Bingham fluids are tooth paste, tomato paste, ketchup and hand cream.

Pseudoplastic with a yield stres: These fluids have a nonlinear shear stress versus shear rate relationship in addition to the presence of a yield stress such as filled polymer melts.

2.1.2. Time-dependent flow behaviour

Fluids mentioned above are not depend on time but some non-Newtonian fluids, thixotropic and rheopectic, are also depend on time.

Thixotropic Fluid: Some materials such as yoghurt, mayonnaise, salad dressing or margarine becomes more fluid with increasing time of applied force. Thixotropic behavior can be determined by using loop test. In this method, shear rate increases continuously from zero to maximum value and after reaching this point it starts to decrease continuously back to zero. Because of the breakdown of the fluid structure which occurs during the test one obtains a flow curve with a hysteresis loop as seen in Figure 2.3(a).

Rheopectic Fluid: Apart from the positive thixotropy described above, there is also negative thixotropy or anti-thixotropy called rheopexy. These fluids exhibit a reversible increase in shear stress with time at a constant shear rate and fixed temperature as shown in Figure 2.3(b). Some clay suspensions show rheopectic behavior.

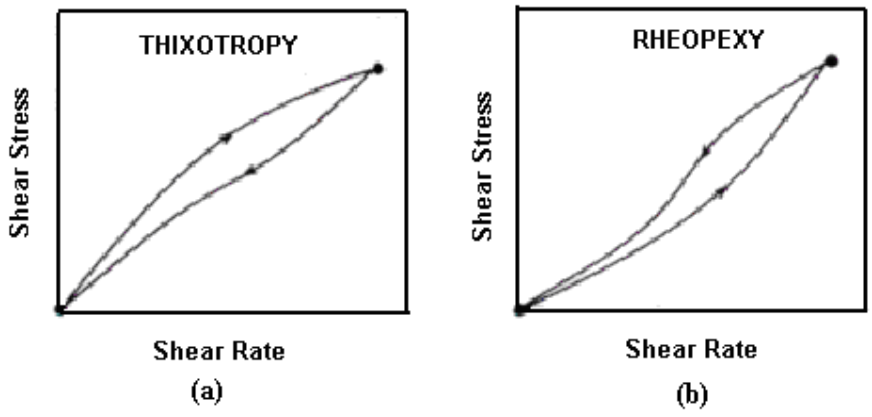

Figure 2.3: The flow curves of thixotropic and rheopexy fluid.

2.2. Shear Rate-Dependent Viscosity Laws

Viscosity models are too important for flow analysis. They are used to fit the shear rate dependence of viscosity. Using some laws are explained shortly below.

2.2.1. Power Law

Power law described by a linear relationship between the logarithm of the shear stress and the logarithm of the shear rate. It is the simplest model to define for shear thinning behavior. The power law model requires two parameter for fluid characterization as seen in Equation 2.5.

$$\eta = k \dot{\gamma}^{n-1} \tag{2.5}$$

and logarithmic form of model is given in Equation 2.6.

$$\log \eta = \log \mathrm{k} + (\mathrm{n}-1) \log \dot{\gamma} \tag{2.6}$$

If $\log(\eta)$ is plotted against $\log(\dot{\gamma})$, the slope of the curve is equal to the (n-1) and the intercept is equal to the $\log \mathrm{k}$. Where k and n are rheological parameters. n is called power law exponent that describes the degree of deviation from Newtonian behavior and k is consistency index of the fluid.

According to power law model, if n = 1 Newtonian fluid's flow curve and if n < 1 shear thinning fluid's flow curve and if n >1 shear thickening fluid's flow curve is obtained. The usual range of power-law exponent values is between 0.8 (for polycarbonat) and 0.2 (for rubber compounds), and for various grades of polyethylene, the range is $0.3 < n < 0.6$ [5].

For example for shear thinning fluids (n<1) the model predicts;

$\eta \to \infty$ for $\dot{\gamma} \to 0$ and $\eta \to 0$ for $\dot{\gamma} \to \infty$

This mean that shear rate approaching zero and approaching infinity the value of η approaches a constant finite value. These values are the zero shear viscosity η_0 and the infinite shear viscosity η_∞, respectively, and in the case of n<1 one has $\eta_0 > \eta_\infty$.

Figure 2.4 show typical flow curve of a shear thinning fluid [6].

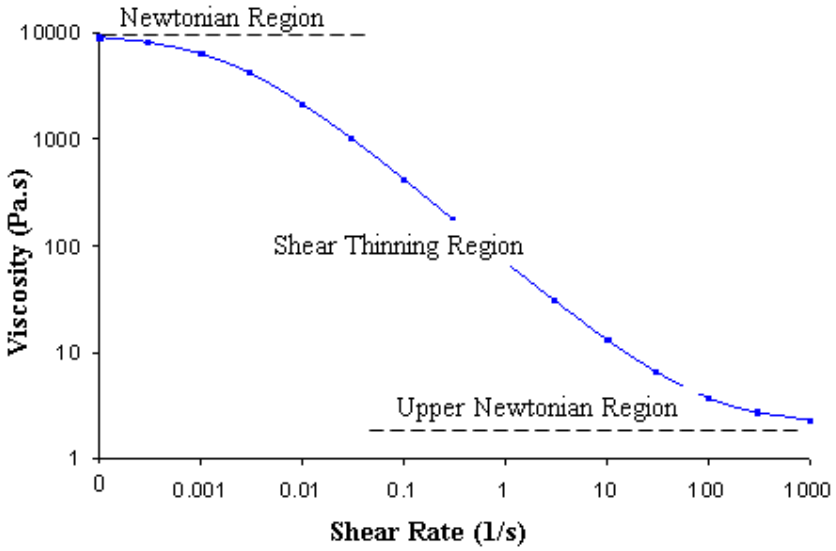

Figure 2.4: Viscosity profile for a polymer melt.

As seen in Figure 2.4, there are three regions on plot;

- The first region, at low shear rate, is called Newtonian region and in this region viscosity is named zero shear rate viscosity.
- The second region, at intermediate shear rate, is called Power law region. In this region, a straight line is obtained on a log-log plot of viscosity against shear rate.
- The end of the curve, at high shear rate, is called upper Newtonian region and characterized by a constant infinite shear rate viscosity.

The power law is commonly used to describe the viscous behavior of polymeric materials, such as polyethylene, with shear rates greater than 2 or 3 decades. If the behavior at low shear rates needs to be fitted as well, the Bird-Carreau or Cross law will capture the plateau zone of the viscosity curve for low shear rates better than the power law [7].

2.2.2. Bird-Carreau Law

The Bird-Carreau law is commonly used when it is necessary to describe the low-shear-rate behavior of the viscosity and it is given in Equation 2.7.

$$\eta = \eta_\infty + (\eta_0 - \eta_\infty)(1 + \lambda^2 \dot{\gamma}^2)^{\frac{n-1}{2}} \quad \textbf{(2.7)}$$

Where η_∞ is infinite-shear-rate viscosity, η_0 is zero-shear-rate viscosity, λ is natural time and n is power law index.

2.2.3. Cross Law

Like the Bird-Carreau law, the Cross law is commonly used when it is necessary to describe the low-shear-rate behavior of the viscosity.

The Cross law for viscosity is given in Equation 2.8.

$$\eta = \frac{\eta_0}{1 + (\lambda \dot{\gamma})^m} \quad \textbf{(2.8)}$$

Where η_0 is zero shear rate viscosity, λ is natural time and m is cross-law index and equal to 1-n.

2.2.4. Carreau-Yasuda Law

The equation of Carreau-Yasuda law shown in Equation 2.9.

$$\eta = \eta_\infty + (\eta_0 - \eta_\infty)[1 + (\lambda \dot{\gamma})^a]^{\frac{n-1}{a}} \quad \textbf{(2.9)}$$

Where η_0 is zero shear rate viscosity, η_∞ is infinite shear rate viscosity, λ is natural time, a is index that controls the transition from the Newtonian plateau to the power law region and n is power law index.

Of course, there are many other models describing above but the models presented above are the most using ones for industrial applications.

2.3. Viscosity Parameters

The effect of shear rate on viscosity has been discussed above. However, there are some other variables that affect the viscosity such as temperature, pressure, intermolecular bonding, chain flexibility, structure of repeat unit, additives and its concentrations, crystallinity and molecular weight distribution. The effect of these factors is generally not as strong as the effect of shear rate but some times, the effect of temperature, pressure or molecular weight distribution connot be neglected.

2.3.1. Viscosity Temperature Relationship

According to the literature, when the viscosity is plotted against shear rate at several temperature, the curve generally decreases with increasing temperature because of thermal motion of molecules.

As seen in Figure 2.5, the shape of the viscosity curve of polymer melts remains approximately similar at different temperatures [8]. Because of this, viscosity versus shear rate data can be show by a referance curve. In this case, if we know the ratio of the zero shear viscosities at the two temperatures, we can find the complete flow curve at desired temperatures. To determine the effect of temperature on the viscosity, shifting factor (a_t) can be used.

The shifting factor, should be find from the Equation 2.10.

$$a_T = \frac{\eta_0(T)T_0\rho_0}{\eta_0(T_0)T\rho} \qquad \textbf{(2.10)}$$

Where ρ_0 and ρ are densities of the polymer melt at T_0 and T temperatures, respectively.

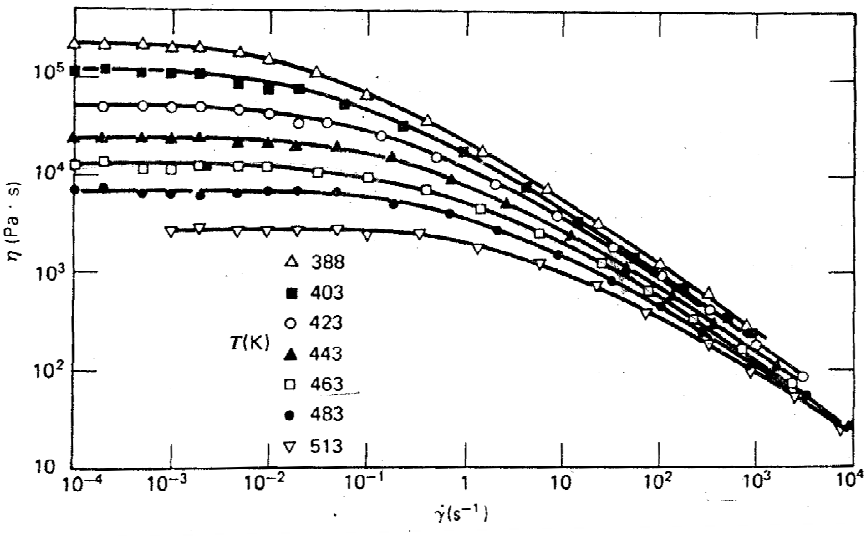

Figure 2.5: Non-Newtonian viscosity of a LDPE melt at several different temperatures.

Presently, there are two commonly used equations, William-Lendel-Ferry (WLF) and Arrhenius Equations, to calculate the temperature dependency of the viscosity.

2.3.1.1. Williams – Lendel – Ferry (WLF) Equation

According to WLF, time-temperature superposition determines the effect of temperature by shifting viscosity curves measured at different temperature onto a single, temperature independent master curve. This equation (Equaiton 2.11) has been used for temperatures between the glass- transition temperature, T_g, and $T_g + 100$ [8].

$$\log a_t = -\frac{C_1'(T - T_s)}{C_2' + (T - T_s)} \qquad \textbf{(2.11)}$$

Here, C_1' and C_2' are constants and T_s is standard temperature.

If T_s is chosen as the glass transition temperature for practical calculations, in this case C_1'=17,44 and C_2'=51,6 for a wide range of polymers.

2.3.1.2. Arrhenius Equation

When the temperatures are more than 100 ºC above T_g, Arrhenius equation (Equation 2.12) is used.

$$a_T = \exp\left[\frac{\Delta E}{R}\left(\frac{1}{T}-\frac{1}{T_0}\right)\right] \quad \textbf{(2.12)}$$

Where ΔE is activation energy and R is the universal gas constant. According to the some studies, $\Delta E/R$ values are found to be $4{,}5\times10^{3\,o}K$, $2{,}83\times10^{3\,o}K$ and $5{,}14\times10^{3\,o}K$ for LDPE, HDPE and PP, respectively.

2.3.2. Viscosity Molecular Weight Relationship

The size of a polymer molecule is represented by its molecular weight. Molecular weight can be controlled during the manufacturing process. Catalyst, conditions of polymerization, and type of process determine the amount of chain length. However, polymer consists of different lengths so molecular weight is usually expressed as an average value. Molecular weight affects a polymer's melt viscosity or its ability to flow in the molten state. This is shown in Figure 2.6.[9].

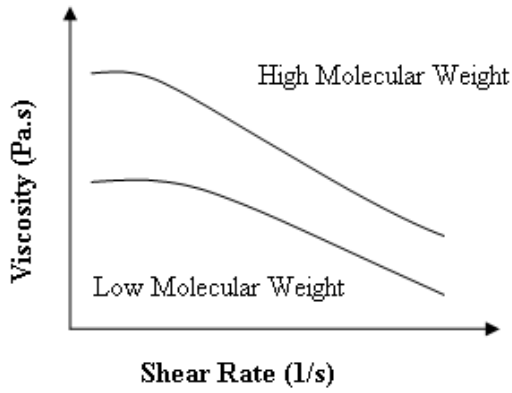

Figure 2.6: The effect of molecular weight on viscosity.

As seen in Figure 2.6, a lower molecular weight polymer will have a lower apparent viscosity than higher molecular weight polymer. At the lower molecular weights, the polymer chains are short and less entangled, therefore, can flow past one another more easly. As the molecular weight continues to drop, the viscosity behaves in a

more Newtonian manner. In addition of this information, broader molecular weight distributions tend to have an earlier onset of shear thinning and a more gradual transition into the power law region.

Narrow distribution have a relatively sharp transition and achieve a steeper slope in the power law region.

At the same time, the zero shear viscosity increases with the average molecular weight as shown in Figure 2.7. Here, $\bar{M}_c$ is critical molecular weight of polymer at which molecular entaglement begins to dominate the rate of slippage of molecules.

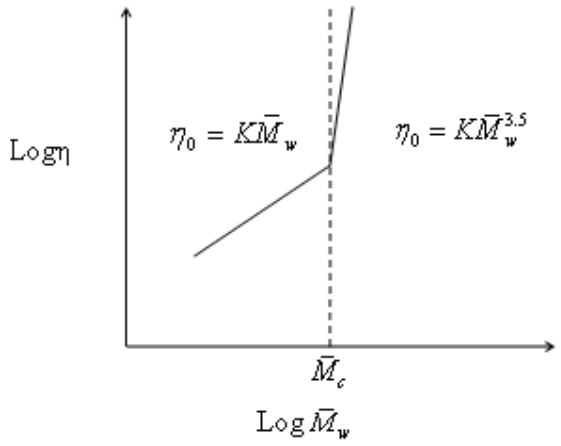

Figure 2.7: Molecular weight- zero shear rate relation ship.

If the weight average molecular weight ($\bar{M}_w$) of a polymer is below $\bar{M}_c$, η_0 is calculated from the Equation 2.13, otherwise η_0 is found from the Equation 2.14 [10-13].

$$\eta_0 = K\bar{M}_w \qquad \textbf{(2.13)}$$

$$\eta_0 = K\bar{M}_w^{3.5} \qquad \textbf{(2.14)}$$

According to the these formulas, below $\bar{M}_c$, η_0 don't affect from the polymer-polymer entanglements. Because at low values of $\bar{M}_w$, the lifetimes of junction points will be short and above $\bar{M}_c$, their lifetime increase with 3,5 power of $\bar{M}_w$.

2.3.3. Viscosity Pressure Relationship

The dependence of viscosity on temperature is generally considered but pressure effects are genereally ignored at low pressure processing such as extrusion, blow molding, or casting. However, this opinion is not valid for high pressure processing such as injection molding, because pressures can up to 100 MPa in injection moulding processes.

In the early 1970s by Cogswell and McGowan investigated the effects of both temperature and pressure on the viscosities of polymeric liquids [14] and then Cogswell studied the effect of pressure on the apparent viscosity of polymer melts such as polypropylene and high-density polyethylene [15]. Cogswell found that an increase in the pressure of a polymer melt was equivalent to a decrease in temperature.

Consequency, the making experiments showed that, the amount of free volume of the material reduse by pressurizing. Hence, the mobility of polymer decreases and viscosity increases. This pressure- viscosity relationship can be explained by using Barus equation (Equation 2.15) [16].

$$\eta = \eta_0 e^{\beta P} \tag{2.15}$$

where η_0 represents viscosity at ambient pressure, P is the gauge pressure, and β is pressure coefficient.

To determine the pressure coefficient, many researchers use a modified capillary rheometer.

2.4. Normal Stress

The stress components occuring during the simple shear of a fluid element are shown in Figure 2.8.[4]. The diagram presents the shear stress component $T_{xy} = \tau_{xy} = \tau$ as well as the symmetric and equal shear stress component $T_{yx} = \tau_{yx} = \tau$ which results from the principle of moment of momentum conversation. The three components of normal stress, T_{xx}, T_{yy} and T_{zz}, are also shown in this figure.

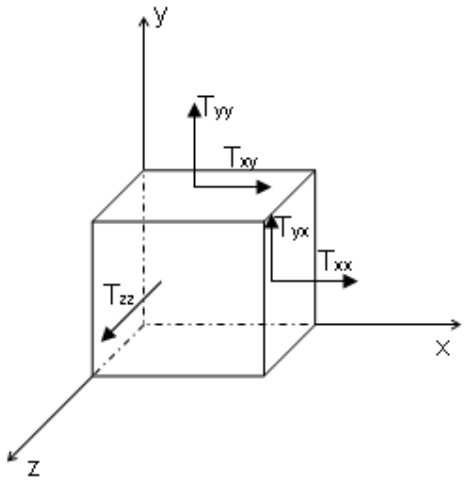

Figure 2.8: Stress components acting on a fluid element in simple shear.

For a Newtonian fluid the normal stress components are equal because a Newtonian fluid, consisting of small molecules, doesn't form any microsucture and is therefore fully isotropic. As shown in Equation 2.16 these components are equal to the hydrostatic pressure (p).

$$T_{xx} = T_{yy} = T_{zz} = -p \qquad \textbf{(2.16)}$$

The negative sign before p results from the convention that the normal stresses are positive when they are oriented externally in respect to the fluid element under consideration, and they cause tension.

On the other hand the pressure p is positive for compression. In the general case of a fluid with microsucture, this structure may exhibit anisotropy. For example, in a polymer solution an interaction occurs between the temporary orientation of the segments of polymer chains on the one hand, and the orientation of the heterogeneous velocity field on the other. This interaction is additionally influenced by the thermal motions of the fluid. In a fluid at reast the segments of polymer chains would be influenced by the thermal motions only, hence they would have a completely random orientation. The velocity field introduces, however, a privieged orientation, and in consequence a statistical segment takes up an equilibrium position. This leads to the anisotropy of the system resulting in additional force components, which are different in different directions. Hence the normal stress components are not equal to each other (Equation 2.17)

$$T_{xx} \neq T_{yy} \neq T_{zz} \neq -p \quad \textbf{(2.17)}$$

In classical fluid mechanics it is assumed that the hydrostatic pressure is equal to the arithmetic mean of the normal stress components for Newtonian fluids (Equation 2.19).

$$p = \tfrac{-1}{3}\left(T_{xx} + T_{yy} + T_{zz}\right) \quad \textbf{(2.18)}$$

And the normal stress components can be defined by Equation 2.19-2.21.

$$T_{xx} = -p + \tau_{xx} \quad \textbf{(2.19)}$$

$$T_{yy} = -p + \tau_{yy} \quad \textbf{(2.20)}$$

$$T_{zz} = -p + \tau_{zz} \quad \textbf{(2.21)}$$

Here, the rheologically undefined quantity, p, is eliminated because of being interested in rheological quaintities only. This may be accomplished by simple subtraction. Hence, first normal stress diffrecence is definedin Equation 2.22.

$$N_1 = T_{xx} - T_{yy} = -p + \tau_{xx} + p - \tau_{yy} = \tau_{xx} - \tau_{yy} \quad \textbf{(2.22)}$$

And the second normal stress difference in Equation 2.23.

$$N_2 = T_{yy} - T_{zz} = \tau_{yy} - \tau_{zz} \quad \textbf{(2.23)}$$

and finally the third normal stress in Equation 2.24.

$$N_3 = T_{xx} - T_{zz} = \tau_{xx} - \tau_{zz} \quad \textbf{(2.24)}$$

As seen above, the third normal stress is equal to the sum of the the first and second normal stress differences.

It follows from experimental investigations that the first normal stress difference (N_1) is generated only in fluids which exhibit elasticity. For very elastic fluids the first normal stress difference may become even larger than the shear stress. In this situation, the first normal stress can not be neglected.

The ratio of N_1 to τ is used to characterize quantitatively the fluid elasticity. For this purpose the recoverable shear is defined as $\frac{N_1}{2\tau}$. If the recoverable shear exceeds 0.5 the fluid is regarded as highly elastic.

All the experimental data show that N_1 is positive. On the other hand, N_2 is zero or negative and smaller than N_1 values. Therefore, N_2 is taken equal to zero in practical applications.

It is an experimental fact that during the laminar shear flow of a viscoelastic fluid a force in the direction normal to the direction of flow occurs. Forexample, in the simple shear between parallel plates the normal force tries to push the plates apart. The occurence of this force may be explained by the Equations 2.25-2.27.

Using above equations, τ_{xx}, τ_{yy} and τ_{zz} can be found as

$$\tau_{xx} = \frac{2N_1 + N_2}{3} \qquad \textbf{(2.25)}$$

$$\tau_{yy} = -\frac{N_1 - N_2}{3} \qquad \textbf{(2.26)}$$

$$\tau_{zz} = -\frac{N_1 + 2N_2}{3} \qquad \textbf{(2.27)}$$

In the parallel plates, the force acting on the upper moving plate is given Equation 2.28

$$F = -\tau_{yy} = \frac{N_1 - N_2}{3} \qquad \textbf{(2.28)}$$

According to the this equation, F is positive and acts in the upward direction because $N_1 > 0$ and $N_2 \leq 0$.

2.4.1. Normal Stress Effects

Normal stress play a major role in a number of industrial processes like extrusion or fiber spinning. The best known normal stress effects are the rod climbing and die swell.

2.4.1.1. Rod Climbing (Weissenberg Effect)

This phenomenon occurs when a rotating rod is placed in a pot containning viscoelastic fluid with the axis of the rod perpendicular to the free surface of the fluid. In Newtonian fluids, centrifugal forces generated by the rotation push the fluid away from the rod. But in non-Newtonian fluids, normal forces are stronger than centrifugal forces and drive the fluid inward toward the rod as seen in Figure 2.7 [17].

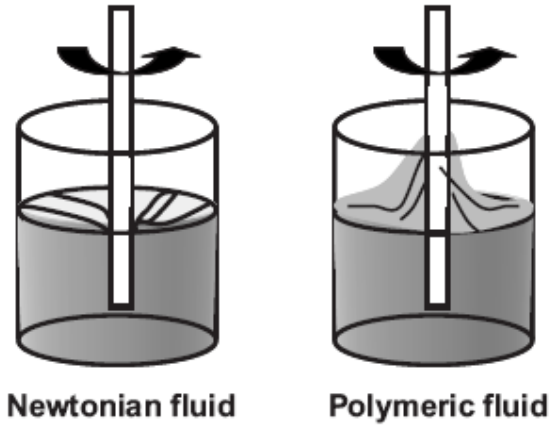

Figure 2.7: Weissenberg effect.

This phenomenon generally seen in rotational viscometric studies at high speeds.

2.4.1.2 Die Swell

As a non-Newtonian fluid flows out of a capillary, the extrudate diameter is larger than the hole which it emerged (Figure 2.8 [18]). This phenomenon is called die or extrudate swell which is a characteristic of the elastic behaviour of viscoelastic fluids.

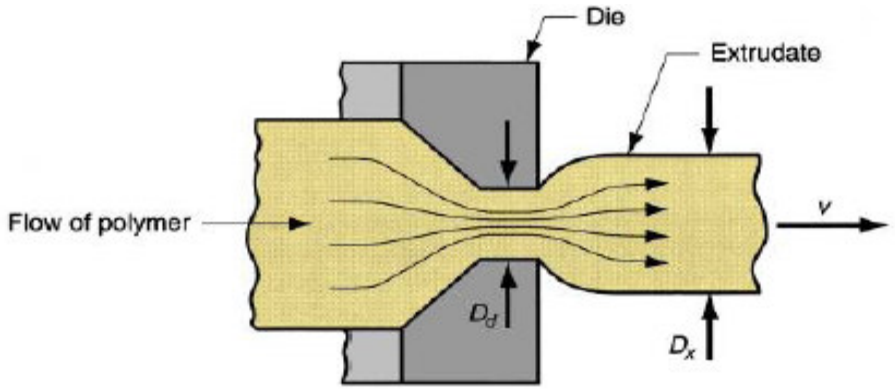

Figure 2.8: Die swell.

Die swell is related with applied stresses. Graessley et.all found that die swell is correlated with wall shear stress, because the end pressure drop is an important characteristic for the elastic energy stored in the melt during capillary flow and pressure drop increases non-linearly with increasing shear stress at the constant test temperature [19].

Changing velocity profiles are another reason for this phenomenon. As known, fluid velocity profiles are hyperbolic in the capillary but they becomes flat out of the capillary and a uniform velocity across the extrudate diameter being reached.

A number of study have been done to calculate normal stress from the die swell data. One of them is Taner's study. Die swell shear stress relationship is commonly explained by Taner's equation which is given in Equation 2.29.

$$\frac{D_p}{D_c} = 0,1 + \left[1 + \frac{1}{2}\left(\frac{N_1}{2\tau_w}\right)^2\right]^{\frac{1}{6}} \qquad \textbf{(2.29)}$$

Where D_p is the diameter of the extrudate, D_c is the capillary diameter, N_1 is first normal stress difference which is explained before and τ_w is the shear stress at the wall. As seen in Tanner's equation, die swell can be correlated to N_1.

3. SOME COMMONLY USED RHEOMETERS

To design or optimization of processing equipment and predict product performance, knowledge of the rheological properties of materials such as rubber, plastics and paints is important. Hence, many measurement techniques have been developed to determine flow properties. These instruments are generally named to as rheometers. The rheometers that will be briefly desribed in the next few sections are the capillary rheometer, the melt indexer and rotational rheometers.

3.1. Poiseuille and Couette Flows

Flows used in rheometers may be divided into two classes, Poiseuille (pressure driven) and Couette. In Poiseuille flow, the walls of the system are stationary and the flow is generated the application of external pressure. In Couette flow, there ise no pressure difference, but one of the walls of the system is moved so it is theoretically the best geometry for a rotational rheometer. In fact the fluid is dragged along with the wall therefore couette flow also called drag flow.

The Poiseuille and Couette flows are shown in Figure 3.1 [4].

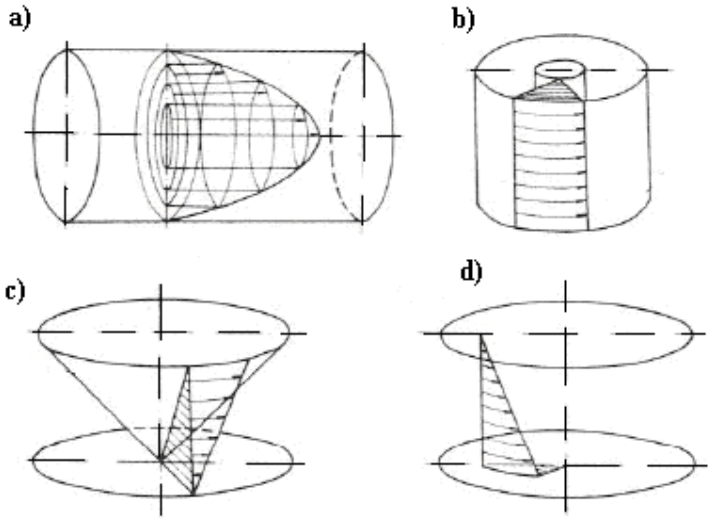

Figure 3.1: The Poiseuille and Couette flows.

These flows that are very important for practical applications. Such as

a) Poiseuille flow in a cylindrical tube

b) Couette flow between two coaxial cylinders

c) Couette flow between a cone and a plate

d) Couette flow between two paralel plates

As seen Figure 3.1. Couette flow occur in rotational and Poiseuille flow occur in capillary rheometer. Both types of rheometer can determine flow curve of a fluid, however, there are some specific advantages and disadvantages between them.

3.1.1. Capillary Rheometer

The first capillary viscosimeter was designed by Hagen in 1839. This instrument is still the case with the common glass capillary viscometers which are used for lower viscosity liquids [20]. Then Couette has introduced the coaxial cylinder instrument in 1890. Until this time, capillary rheometer was the only measuring technique and does not never lost its importance although many new techniques have been developed.

The capillary rheometer is essentially a ram extruder, whereby a piston is accurately driven down a high precision, heated, bore. Inside the bore is the molten polymer, and under the action of the driven piston, the melt is extruded through a die of known geometry. Capillary rheometry is an attractive technique because of several reasons. Firstly, it can test flow behaviour of materials over a wide range of shear rates and temperatures. Secondly, some processing problems such as melt fracture, die swell, etc, can be predicted with capillary rheometer. Thirdly, the data which are derived from testing can also be modelled mathematically with some simulation software packages such as Moldflow or Polyflow. Finally, many material can be tested with capillary rheometer. Essentially almost all thermoplastics used in production such as Polyethylene, Polypropylene, Polyamide, Polystyrene, polymer blends, polymer alloys, filled polymers, bio-polymers and also many non-polymeric materials can be tested on a capillary rheometer, such as chocolate, mayonnaise, and oils.

Although the technique of capillary rheometry appears simple, we can come across some problems making the test.

These problems are;

1. No pressure reading.

Sometimes pressure transducer can't read any pressure value. In this case, pressure tap may be bloke because of filling the material or transducer may not sensitive enough to register the pressures.

2. Thermal degradation

If material have been longer than its residence time in the barrel, the thermal degredation may occur. In which case, the residence time of the material should be shortened. A thermal degradation test can be performed to determine the maximum residence time in the rheometer.

3. Chemical degredation

If there are bubles on the extrudate, the chemical degredation has been occur because polymer molecules are relatively unstable chemically, especially in the molten form. This is an important problem using hydrophilic polymers, such as polyamides, polyesters and biological polymers because of moisture absorption.

4. Copressibility/ density effects

Polymers are assumed incompressible at used equations but in some situations, testing very tough materials, used die with a very large L/D ratio, high pressure can occurs then material density can change flowing through the die. This effect is seemed in Bagley plot so that curved lines rather than straight lines can indicate the possibility of pressure effects in the viscosity.

5. Shear heating

When the polymer melt is sheared at high shear rates, shear heating occur due to viscous dissipation near the capillary wall. This heat will lower the viscosity near the wall and make the fluid appear more shear thinning. The Nahme number (Na) is the critical parameter for estimating the importance of shear heating in rheomecry. It determines how much the temperature rise will affect the viscosity. For capillary flow;

$$\mathrm{Na} = \frac{\beta \tau \dot{\gamma} R^2}{4k} \qquad \textbf{(3.1)}$$

where k is the thermal conductivity and β is the temperature sensitivity of viscosity. When Na≥1 significant errors occur in capillary measurements as a result of viscous dissipation.

3.1.2. Melt Flow Index

The Melt Flow Index (MFI or latterly known as the Melt Flow Rate, MFR) is a simple ram extruder as seen in Figure 3.2 [21]. The melt flow index is the mass of the polymer that extrudes in 10 minutes. Therefore viscosity of material can be understood. Forexample, high melt flow index indicates low viscosity or low melt flow index indicates high viscosity.

In MFI instrument, a polymer sample is, placed in a barrel, heated to the its testing temperature, and extruded through a capillary die. In this case, typical weights, range of 1,2–21,6 kg are used to drive the flow of the polymer through the capillary.

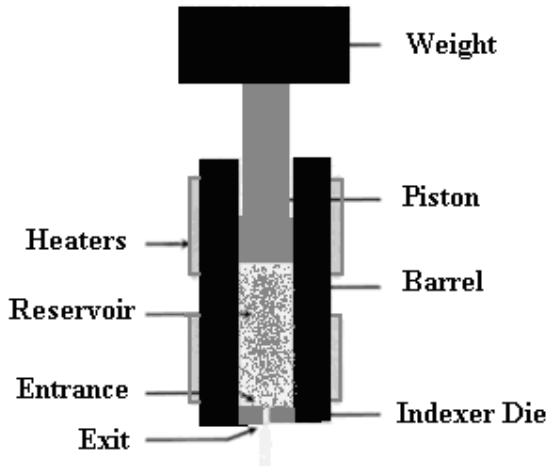

Figure 3.2: Schematic of a melt index.

Melt flow rate gives roughly information about the molecular weight and processability of the polymer. MFI value is inversely related to molecular weight. For example, if polymer has a low molecular weight, flows through the die easily. In this case, MFI value will be high.

Figure 3.3 gives comparison of the MFI to other polymer processing and measuring techniques [22]. As seen this figure, the MFI test conditions are far from the most processes but capillary rheometer not.

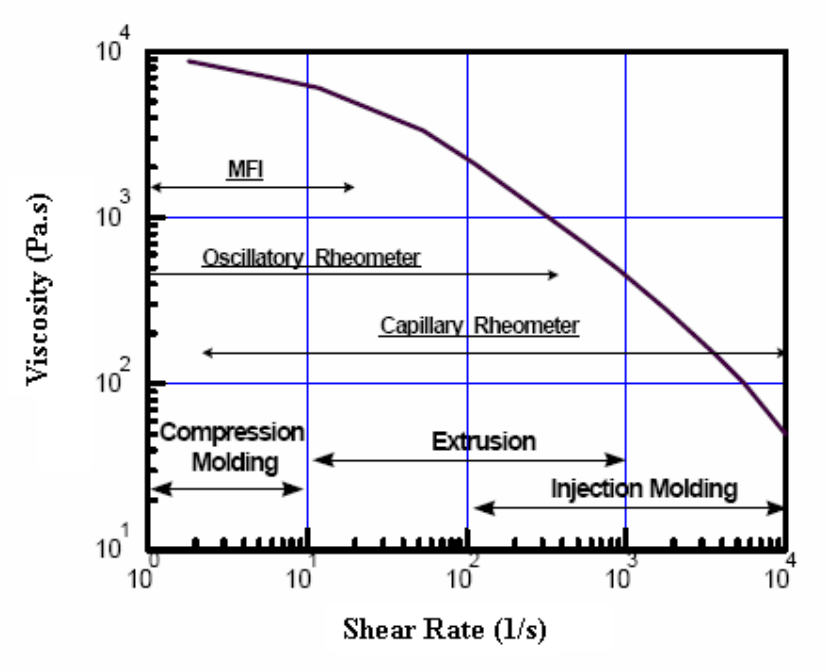

Figure 3.3: Comparison of the MFI to other polymer processing techniques.

Another disadvantage is that MFI represents results at only a single point of the viscosity curve. In this situation tested materials which have same MFI value can be different materials. Figure 3.4(a) shows the rheology curve for a typical linear low density polyethylene (Resin A) and one of the more homogeneous metallocene catalyzed octene copolymers (Resin B) [23]. In this case standard MFI measurements on the two polyolefin polymers show that they both have the same melt flow rate of 1 gram/10 minutes. Figure 3.4(b) shows a comparison of the polymer's calculated average molecular weights, determined from size exclusion chromatography. Consequently, although they have similar average molecular weights, reflected in the MFI, they have significantly different molecular weight distributions and this difference is seen under the processing conditions. For example, while injection molded parts are produced from the resin A under the same molding conditions resin B don't produce.

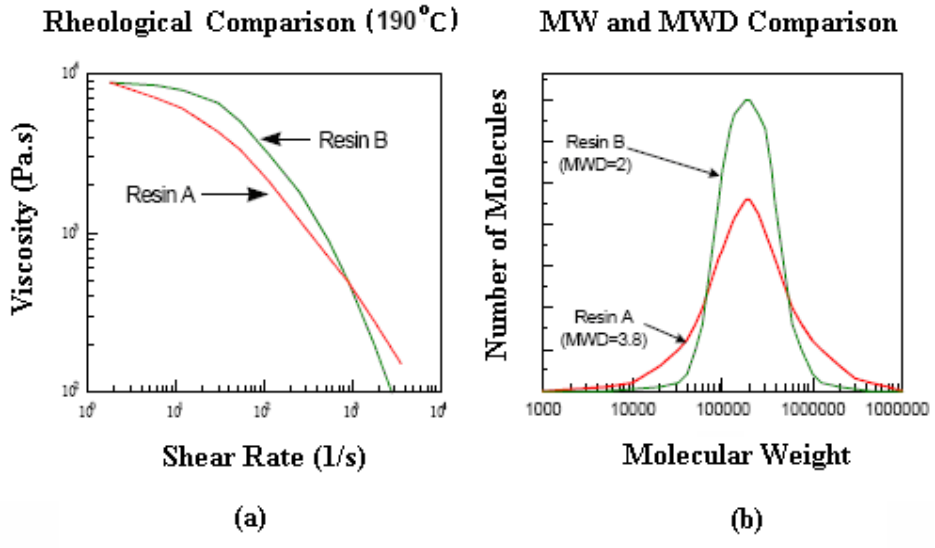

Figure 3.4: Comparison of two resins with MFI = 1.0.

Figure 3.5 shows another comparison of three materials, Low Density Polyethylene (LDPE), Linear Low Density Polyethylene (LLDPE) and Metallocene Catalyzed Polyethylene (MCPE) , which have similar melt flow rates [23]. Melt flow index would predict that all of these materials with different polymer structures would require similar processing conditions.

However, we can see from the curves that their flow behaviors are quite different at the higher shear rates.

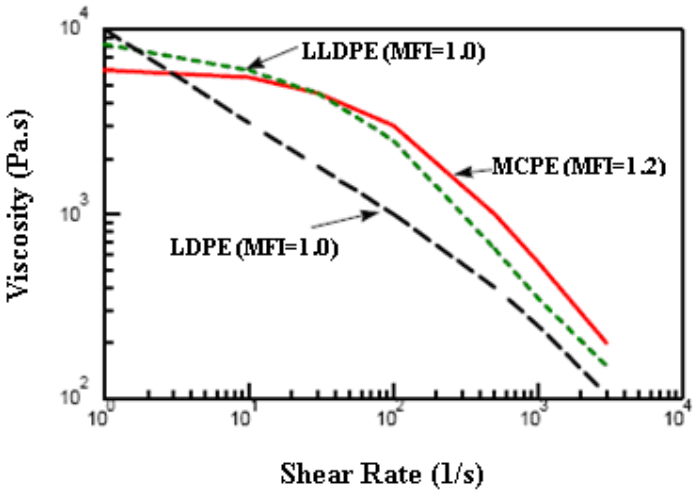

Figure 3.5: Rheological comparison of three resins.

3.1.3. Rotational Rheometers

One type of measuring apparatus is the rotational rheometers. Especially, these rheometers are used for measurement oscillatory strains and a few commercial systems permit measurement of the normal stress. However, measurements with rotational devices become difficult at very high shear stresses because of flow instabilities. This type rheometers are limited to low shear rates (below 10 s^{-1}) [24]. Because the Weissenberg effect tends to draw fluid out of the gap. In addition of this, when small gaps are used, loading and cleaning may be difficult.

Rotational rheometers are available with several different geometries as shown in Figure 3.6 [25].

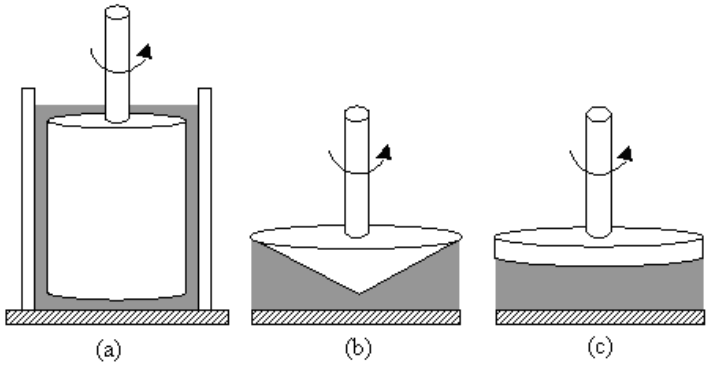

Figure 3.6: Schematic diagram of basic tool geometries for the rotational rheometer; (a) concentric cylinder, (b) cone and plate, (c) paralel plate.

3.1.3.1. Cone and Plate Rheometer

In 1934, Money and Ewart suggested the cone and plate geometry for determining the shear viscosity and Russell used this geometry for normal stress measurements. Today, the cone and plate is probably the most popular rotational geometry for studying non-Newtonian effects.

In this device, the sample, whose rheological properties are to be measured, is trapped between the circular conical disk at the bottom and the circular horizontal plate at the top. The cone is connected to the drive motor which rotates the disk at a constant angular velocity Ω, whereas the plate is connected to the torque measuring device. Figure 3.7 shows a cone and plate rheometer geometry [26].

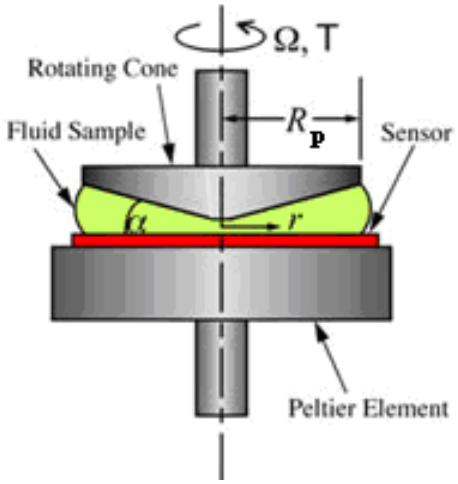

Figure 3.7: Cone and plate rheometer.

As seen in figure the symmetry axes of the cone and the plate coincide and the angle of the cone surface is normally very small (≤ 3°). The cone angles are chosen such that for any point on the cone surface, the ratio of angular speed and distance to the plate is constant. This ensures that the shear rate is constant from the cone tip to the outher radius of the conical disk. Therefore the material properties of the polymeric fluid can be measured at each shear rate directly. This type of rheometers needs a small volume of sample but the maximum shear rate is limited to low shear rates (below $10\,s^{-1}$) because of flow instabilities. Another practical difficulty in rotational rheometers is that of sample loading. With a fluid system the main proplem is ensuring that the sample completely fills the gap in addition and remove bubbles from the sample.

Make some assumptions are used to simplify the calculation of shear rate, shear stress, elasticity etc.

1. Flow is laminar, steady and isothermal
2. The cone angle is very small
3. The cone and plate have the same radius
4. Surface tension effects are negligible

The velocity at any point on the cone surface is proportional to distance from the centre at a given rotational speed (Ω rad s^{-1}). Also the gap width changes linearly with distance from the top of the cone.

Shear rate can be calculated from Equation 3.2.

$$\dot{\gamma} = \frac{\Omega}{\alpha} \tag{3.2}$$

Where α is the cone angle and Ω is a constant rotation speed.

Shear stress is given in Equation 3.3.

$$\tau = \frac{3T}{\alpha \pi R_p^{\,3}} \tag{3.3}$$

Where T is the applied torque and R_p is the plate radius.

Finally, viscosity can be calculated with Equation 3.4.

$$\eta = \frac{\tau}{\dot{\gamma}} \tag{3.4}$$

Also a number of other important parameters such as normal stress, G', relaxation time, can be calculated using measurements over a range of shear rate, shear stress or time.

3.1.3.2. Parallel Plate Rheometer

The parallel plate geometry was suggested by Mooney (1934) then Russell (1946) fist measured normal forces from the total thrust between two plates. Greensmith and Rivlin (1953) measured measured the pressure distribution and Kotaka (1959) used total thrust to study normal stress in polymer melts [20]. The parallel plate rheometer used for measuring the rheological properties of material is similar in principle to the cone and plate rheometer except that the cone is replaced by a smooth circular disk as seen in Figure 3.8 [24].

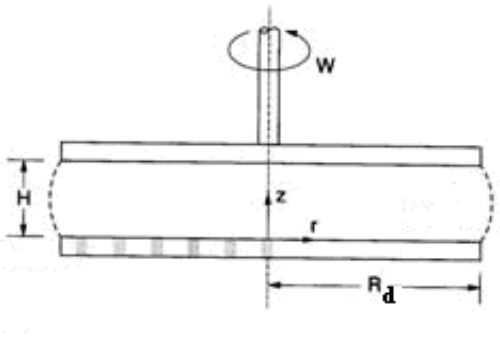

Figure 3.8: Parallel plate rheometer.

Here, the rheological properties are based on the shear rate given in Equation 3.5.

$$\dot{\gamma}_{ap} = \frac{WR_d}{H} \tag{3.5}$$

Where W is the angular velocity (rad/s), R_d is the radius of the disk (cm), and H is the gap between the two parallel disks (cm).

And shear stress is given in Equation 3.6.

$$\tau = \frac{3T}{2\pi R_d^{\,3}}\left[1+\frac{1}{3}\frac{d\ln T}{d\ln \dot{\gamma}_{ap}}\right] \tag{3.6}$$

Where T is the measured torque.

3.1.3.3. Coaxial (Concentric Cylinder) Rheometer

Concentric Cylinders are commonly used for very low viscosity fluids. A cylinder suspended on a torsion bar is placed within a cylindirical cup which is rotated.

The torque, T, on the inner cylinder can be calculated from the Equation 3.7.

$$T = \Omega K \tag{3.7}$$

Where Ω is the rate of rotation and K is the torsion bar constant.

Shear stress is given in Equation 3.8.

$$\tau = \frac{T}{2\pi R_i^{\,2} h} \tag{3.8}$$

Shear rate is given in Equation 3.9.

$$\dot{\gamma} = \frac{2 V_R R_0^{\,2}}{R_0^{\,2} - R_i^{\,2}} \qquad \textbf{(3.9)}$$

Where V_R velocity at R, R_i is radius of inner cylinder and R_0 is radius of outer cylinder. Therfore, the ratio $\tau / \dot{\gamma}$ gives shear viscosity.

3.2. Rheometer Selection

There are many commercial viscometers available on the industry offering a variety of geometries so to choose suitable rheometer, many criterias must be considered. Forexample cost, processing conditions or using aim. These criterias can be explain shortly.

As mentioned before there are two types of rheometers, capillary and rotational, and each serves a different purpose. For example, capillary rheometer is a more improved version of a melt indexer but it is expensive than MFI. Prices change from $30,000 to $45,000 for entry-level, benchtop quality control units up to $100,000 for more advanced models. Also on-line capillary rheometers cost change from $100,000 to $150,000. Capillary rheometers are generally prefered to take shear viscosity data. However, rotational rheometers are especially selected to learn viscoelastic properties. In industry, the concentric cylinder is used mainly for adhesives and coatings. Parallel-plate geometry is used to characterize thermoplastic melts and thermosets and cone-and-plate is used primarily for normal-force testing. At the same parallel-plate or cone and plate rheometers can be used for time creep studies. The cost range of rotational instruments used for plastics is $40,000 to $90,000 [28].

In addition above, for choosing right rheometer also following criterias must be considered;

• The degree of accuracy and precision: quality control (industry) or research measurements (academics).

• Processing shear rate values are also important parameters for selecting rheometer because rheometers run certain shear rate ranges values and these must be near the processing conditions to take true data.

Figure 3.9 gives some processes shear rate values [29].

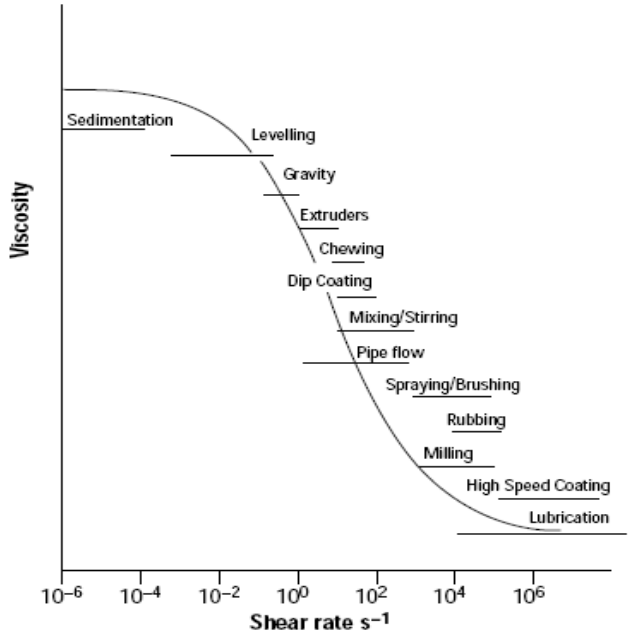

Figure 3.9: Graph of application processes and shear rates.

4. CAPILLARY RHEOMETER

4.1. Types of Capillary Rheometer

There are many commercial versions of capillary rheometer in the literature. Some of them were explained shortly in this chapter.

4.1.1. Controlled Shear Rate

A piston - cylinder capillary rheometer (extrusion rheometer) presented in Figure 4.1 is primarily used to measure melt viscosity of polymers and other viscous materials [30]. In this rheometer, a piston moves with a constant speed inside the barrel. At the bottom of the barrel, there is a die, slit or capillary. Heated blocks around the bore enable to set the desired melt temperature, generally in the range 20-350°C and requiring force is generated by a piston which is generally controlled by a constant speed motor. Pressure transducer is mounted immediately above the capillary dies or mounted on the slit dies to record the pressure drop as the material being tested is extruded through the dies.

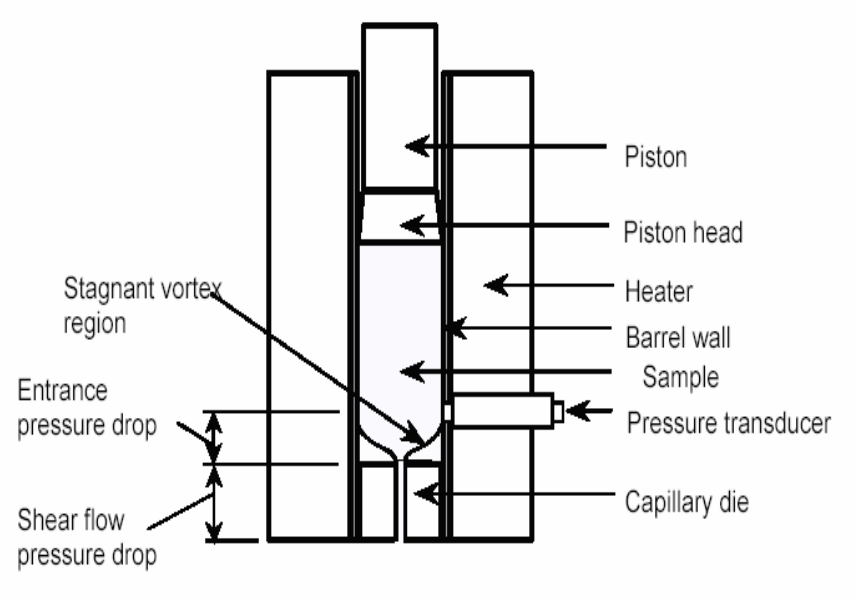

Figure 4.1: Schematic diagram of a capillary extrusion rheometer.

Generally, there are two types of die, slit and capillary, are used in capillary rheometers.

Slit die have a rectangular shape and require three or more pressure transducers to study the pressure profile along the die as seen in Figure 4.2 [31]. This kind of die is generally selected for blow molding applications becase of similarity between them. The main advantage of a slit die is that the pressure transducers can be mounted directly in the die but cleaning is a problem especially near the edges [21].

Figure 4.2: Slit die.

Equations 4.1-4.3 are used for slit die.

$$\dot{\gamma}_{ap} = \frac{6.Q}{H^2.W} \tag{4.1}$$

$$\tau_w = \frac{\Delta P_s.H}{L} \tag{4.2}$$

$$\eta_{ap} = \frac{\tau_w}{\dot{\gamma}_{ap}} = \frac{\Delta P_s.H^3.W}{12.Q.L} \tag{4.3}$$

Where H is the height and W is the width of the slit die.

Round hole or capillary dies are more convenient than slit dies. This kind of die is especially used in pipe processing because of similarity between them. Capillary dies can have vary lenght, diameter and inlet angle. The first two are important for entrance pressure loss corrections and die swell effects and other is important for

special applications. Forexample, flow visualization studies have shown that reducing the entrance angle can delay the onset of flow instability known as melt fracture and die swell can also be reduced. As seen in Figure 4.3, only one pressure transducer is enough for capillary dies [31].

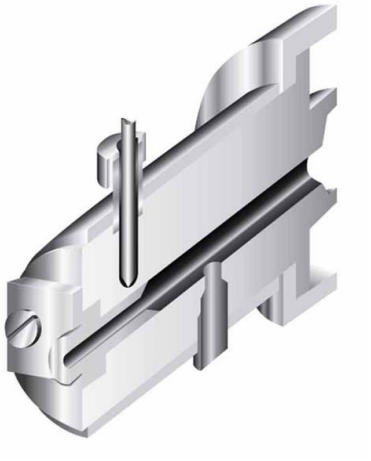

Figure 4.3: Circular die.

4.1.2. Nitrogen Gas Capillary Rheometer

As known many plastics can degrade when in the processing condition because of presence of moisture or oxygen. To test these materials it is usually necessary to dry the sample. To solve this problem, generally the polymer melt is pressurized with a nitrogen gas.

In 1998, a nitrogen gas driven capillary rheometer was designed and constructed by Seyed and Etamad [32].They determined flow behaviour of sodium carboxymethyl cellulose with this system. In 2004, Hans Martin Laun studied on some effects of dissipative heating, hydrostatic pressure and melt compressibility using an automated high precision capillary rheometer which was developed at Basf by Wolfgang Reuther [33]. Also Goettfert which is rheometer producer constructed a twin bore gas griven rheometer. Figure 4.4 shows this rheometer [34]. In this rheometer, the applied controlled pressure is independent of the displacement measurements of the floating pistons in the barrels so frictions in the barrel don't effect the results. However, in this case the nitrogen can soluble in molten polymer under the pressure.

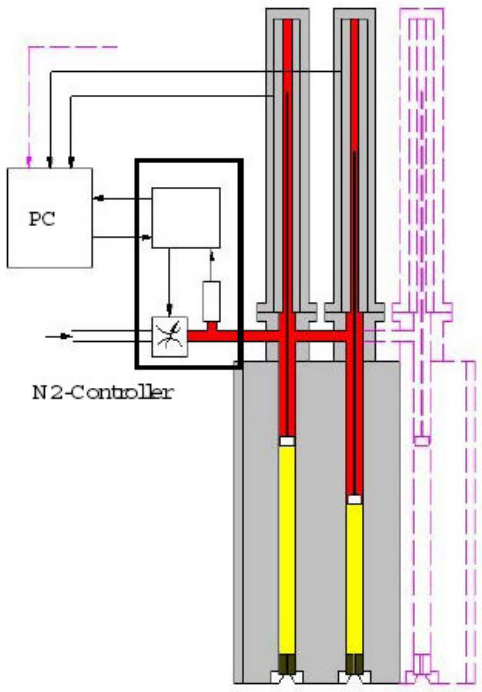

Figure 4.4: Automated nitrogen driven capillary rheometer designed as a twin bore system.

4.1.3. Inline/Online capillary rheometer

These rheometers can measure viscosity directly from the process by mounting the capillary rheometer to one extruder as shown in Figure 4.5.

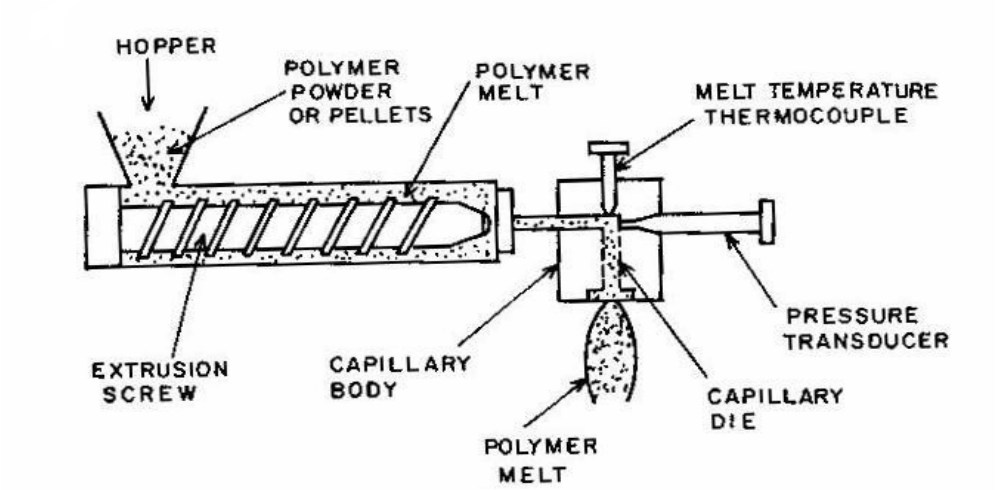

Figure 4.5: Schematic diagram showing the principal features of a constant speed screw extrusion type capillary rheometer.

As known the extrusion process is complex and necessitates long set-up times. Furthermore, combinations of environmental and economic factors require a reduction in waste and energy consumption, and an increase in the use of recycled feed material. A demand for improved process efficiency inevitably leads to the need for better control and appropriate process monitoring. From a control perspective, it is known that the input operating conditions have a significant effect on the quality and rate of the extrudate and the energy efficiency of the process.

Generally, side-stream or on-line rheometers shown in Figure 4.6 are used to measure the in-process melt viscosity. These instruments require a gear pump, which draws off a side stream of polymer melt from the extruder barrel for continuous sampling [35]. The pressure developed by the gear pump forces the melt through a capillary die, which exits to atmosphere. The pressure drop is measured by a wall-mounted transducer in the reservoir prior to the capillary die.

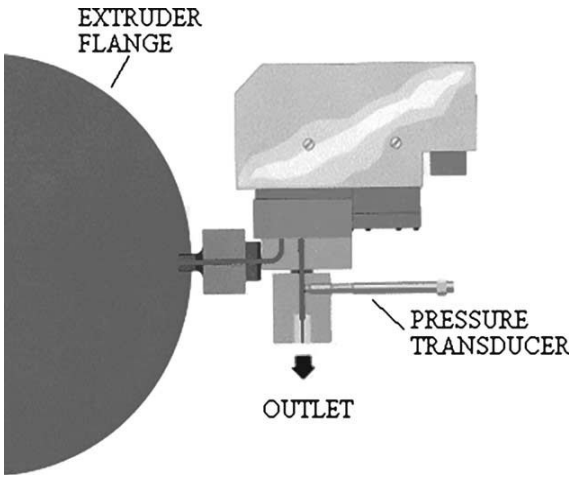

Figure 4.6: Side stream rheometer.

In-line instruments are alternative to 'side-stream' rheometers. These are located between the extruder screw and the die, and incorporate the entire melt stream for sampling. The use of pressure drop measurements along an in-line capillary or slit die to determine the viscosity. Many authors studied on in-line rheometer such as Fleming, Padmanabhan and Bhattacharya, Rauwendaal and Fernandez and Kalyon [36-39]. Moreover, Covas, No´brega and Maia studied on develop a on-line capillary rheometer for measuring rheological properties at different locations along an extruder. Therefore they could determine the evoluation of chemical reactions in the twin screw extruder [40].

Consequently, the above devices are very useful for process and quality control, but each method has its advantage and disadvantages. The laboratory study provide to researching activity however, the data collection period is often too long and reqire trained laboratory personnel. However the speed of data collection with online capillary rheometer is faster than offline measurement. The on-line equipment can provide near real time data but the range of shear rates is somewhat limited. Pressure drop measurement is another disadvantage of on-line rheometer. In on-line capillary rheometer, polymer melt is continuously forced through a die and rheological properties can be determined by measuring its pressure drop and flow rates. However in this method, derive the pressure drop is problem because another capillary with the same diameter and different length is needed to use the Bagley correction explained later and this operation require a complex mecanism. In 1999, Shih-Hsuan Chiu and Sheng-Hong Pong studied on this problem and they estimated pressure drop values in an on-line capillary rheometer using the neural network computer program.

Although the screw extrusion capillary rheometer can be used for rheological studies of polymer melts it is not popular as the piston type capillary rheometers.

In addition all of these, there are also twin or triple bore capillary rheometer. This rheometers requires less test time and effort than single bore rheometer so that two different materials can be tested and Bagley correction is applied easly.

Figure 4.7 shows a triple bore capillary rheometer [41].

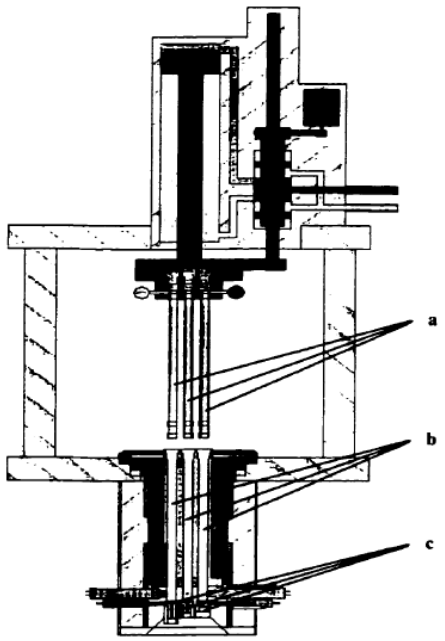

Figure 4.7: Triple bore capillary rheometer.

4.2. Useage Areas Of Capillary Rheometer

In industrial applications, capillary rheometers are used because of some reasons. These were explained shortly.

4.2.1. Material characterization

The main aim of a capillary rheometer is to generate a viscosity-shear rate curve as possible as at a wide range of shear rate for material characterization. This information can be used for

- Selection of suitable material for processing conditions.
- Effect of additives, adding or changing fillers in a material.
- Process equipment design.

4.2.2. Thermal Stability

Thermal stability determine how long material can be maintained at a specific temperature before it begins to degrade. This information is critical for process designers and can be used to test the performance of stabilization-additive packages. Capillary rheometer can also used to determine thermal stability of a material. Forexample, Huang and Xu studied on thermal degradation of PP in a capillary

rheometer [42]. They measured MFI values of samples after shearing and heating treatment to characterize the molecular weight change and they found an increase in MFI at high temperature and longer time heating.

4.2.3. Melt Density

Melt density of a material also determined with a capillary rheometer. For this measurement, sample is loaded into the capillary rheometer then some material is purged through the die to ensure that no air is in the system at the working temperature. Initial position of the piston is noted and sample is revoved from die. All extruded sample is collected when the piston stops. The final position of the piston is noted to determine how far it traveled. The distance traveled is multiplied by the cross-sectional area of the piston to get the volume of the material extruded. Then, extruded sample is weighed and this weight is divided by the volume to get the sample density.

4.2.4. Process Control Optimization

As mentioned before, rheological information is valuable tool for setting up production machines. When a new material is received into a process, a capillary rheometer can provides a picture of the resin and its quality control limits. This information can then be correlated with the processing conditions established when the processis set up correctly. If the flow curve falls out side of the limits, the material can be returned or a new quality control curve generated to correlate to the new machine conditions.

4.2.5. Melt Tensile Tests

The extensional properties of a material is very important for polymer processes such as film blowing, fiber spinning, and blow molding. Generally, two methods are used for measuring extensional viscosity of polymer. In the capillary rheometer applications, Rheotens or melt tensile tester apparatus, shown in Figure 4.8, used to determine the extensional viscosity. Rheotens is a device which pull on a melt strand as it is extruded from the capillary die and measure the force to generated melt extension.

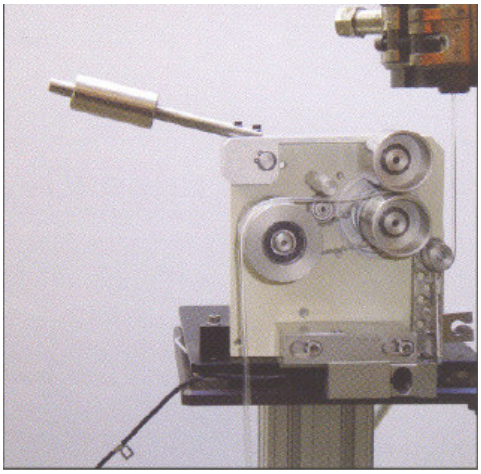

Figure 4.8: Rheotens.

These instruments are capable of measuring very small forces and can generate the extensional strain rates found in many processes. Especially, these are used for qualitative testing of materials to process or quality control.

Extensional rate isgiven in Equation 4.4.

$$\dot{\varepsilon} = \frac{2\pi\nu R_w}{\mathrm{H}} \ln\left[\frac{8\pi\nu R_w}{\dot{\gamma}_a R}\right] \qquad \textbf{(4.4)}$$

Where ν, R_w are the annular velocity and radius of the roller, respectively. H is the distance of the capillary to the roller and R is the radius of the die and $\dot{\gamma}_a$ is the apparent shear rate.

The normal stress difference is given in Equation 4.5.

$$\tau_e = \frac{8\mathrm{v}R_w\mathrm{F}}{R^3\dot{\gamma}_a} \qquad \textbf{(4.5)}$$

Where F is the tensile force determined by the tension transmitted through the melt strand to the take up wheels. Hence, the extensional viscosity is given in Equation 4.6.

$$\eta_e = \frac{\tau_e}{\dot{\varepsilon}} \qquad \textbf{(4.6)}$$

The other method is used entrance pressure drop data for determining extensional or elongational viscosity. Cogswell considered that there are two component, shear and extensional, in the contraction area and by assuming that the pressure drop can be separated into shear and extensional components. Cogswell calculated extensional viscosity using these pressure drop data.

The extensional rate is given in Equation 4.7.

$$\dot{\varepsilon} = \frac{4\dot{\gamma}_a^2 \eta_{ap}}{3(n+1)\Delta P_{ent}} \tag{4.7}$$

and the normal stress difference is given Equation 4.8.

$$\tau_e = \frac{3(n+1)\Delta P_{ent}}{8} \tag{4.8}$$

Where n is the power-law index and η_{ap} is the apparent viscosity and $\dot{\gamma}_a$ is the apparent shear rate in the capillary.

If τ_e and $\dot{\varepsilon}$ are known, extensional viscosity can be calculated from the Equation 4.9.

$$\eta_e = \frac{\tau_e}{\dot{\varepsilon}} = \frac{9(n+1)^2 \Delta P_{ent}^{\ 2}}{32\dot{\gamma}_a^2 \eta_{ap}} \tag{4.9}$$

As seen in above, Cogswell's analysis requires shear viscosity data. If know the shear viscosity parameters, Cogswell's equations permit the calculation of the extensional viscosity.

4.2.6. Thermal Conductivity Measurement

The thermal conductivity of polymers is important property for the cooling of mouldings, which is critical in determining cycle times since polymers have low thermal conductivities.

Commercial software requires a range of heat transfer parameters to optimize polymer processing and these parameters can be measured with a capillary rheometer. For this aim, Göttfert Company designed a triple bore capillary

rheometer, shown in Figure 4.9. One single bore for measurements of the thermal conductivity while the second and the third bore for routine viscosity tests.

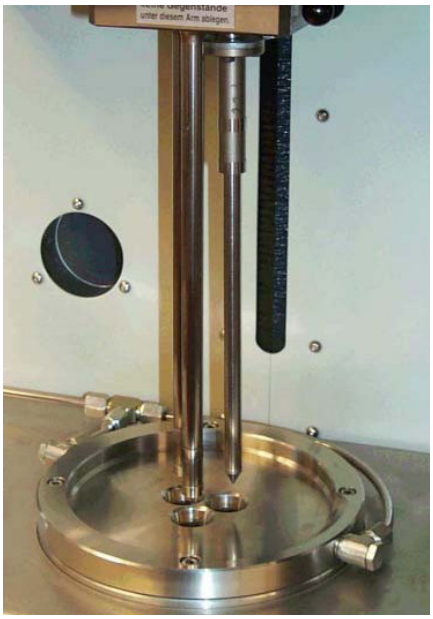

Figure 4.9: Triple bore capillary rheometer.

Using thermal conductivity probe has a thermocouple in the centre as shown in Figure 4.10.

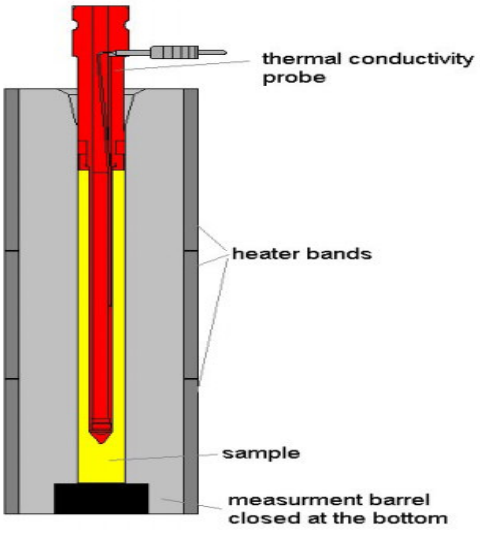

Figure 4.10: Thermal conductivity probe.

In this test, once polymer granules are filled into the barrel. The thermal conductivity probe is moved into the barrel and measure increase of temperature. Therefore, thermal conductivity is calculated from the temperature increase [43].

4.2.7. Wall Slip Effect

Extudate distortions or melt fracture phenomena which shown in Figure 4.11 is one of the most important problem especially for film and pipe extrusion process where surface quality is important [44]. Both industry and academia have expended a great effort to understand the causes of this phenomena.

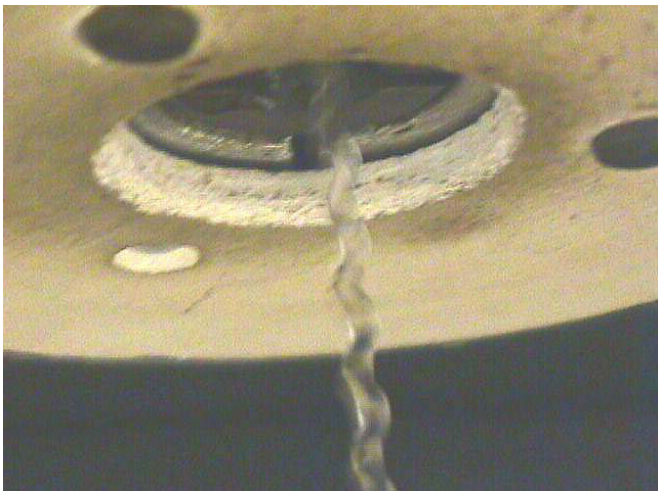

Figure 4.11: Photograph of the severe melt flow instability.

According to the literature, the formation of a lubricating layer adjacent to the wall due to migration effects or loosing adhesion with the wall may be reasons for occuring melt fracture [45]. Macosko commented that this migration is more greater at higher shear rates [20]. Also some studies show that slip behaviour is influenced from the wall surface texture and material of construction. For example, Chen, Kalyon, D.M and Bayramlı found that slip behaviour of low density polyethylene was influenced by both the material of construction and by surface roughness [46].

In addition, Ramamuthy, Kalika and Denn suggest that melt fracture occurs exceeding a critical shear stress due to the adhesion failure [47-48].

Most of the studies on the melt fracture of polymers focused on the behavior of polyethylenes. Experiments have showed that melt fracture behaviour of PE is complicated. For example, Figure 4.12 shows a typical flow curve for a linear polethylene which is determined by a capillary rheometer under constant piston speed operation. As seen in graph, there are four different flow regions. In region A, extrudate surface is smooth and in region B where applied shear stress greater than a critical value τ_{c1} a small amplitude periodic distortions appear on extrudate surface

and in region C, flow becomes unstable. Finally, extrudate surface becomes more unstable in region D [49].

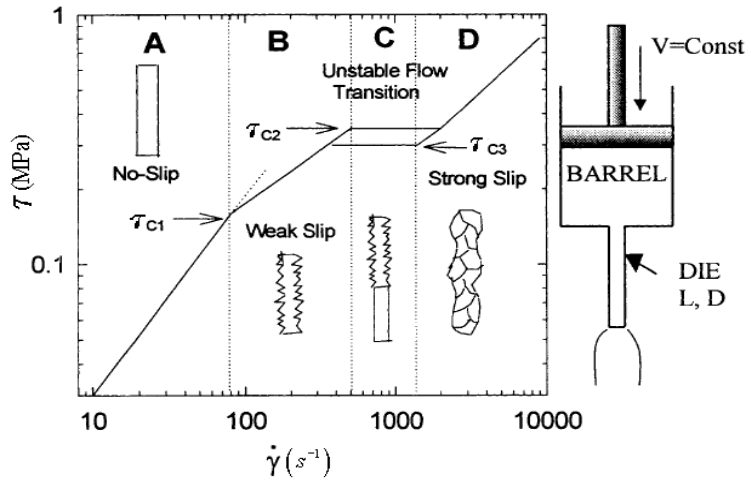

Figure 4.12: A typical flow curve of a linear polyethlene as determined by a capillary rheometer.

According to this study, wall slip occured when the wall shear stress exceeds critical value [50]. Another study has been done for PE by Sornberger [51]. Sornberger divided the flow curve of linear PE into five stages. In the first stage a smooth cylindrical extrudate was seen. In the second stage, a small disturbance was seen on the extrudate, which is called sharkskin or surface melt fracture. In the third stage, a periodical pattern occured on the extrudates. This flow is generally called a spurt flow. Consequently, in the fifth stage, a very disordered was observed on surface. However, melt fracture behaviour of PP is simpler than that of PE. Ui, Ballenger, Akay Fujiyama and Kawasaki studied the melt fracture behavior and a critical wall shear stress value of PP [52-55]. Generally, they found critical shear stresses for the onset of melt fracture ranging from 0,13 to 0,2 MPa. Also Huang and Tao [56] studied on melt fractures behaviour of a high molecular weight PP in a capillary rheometer. They observed that melt fracture has became noticeable when the apparent shear rates exceeded 100 (1/s), and regular patterns appeared on extrudates between 100 and 1000 (1/s). They used the plot which the apparent shear stress versus the apparent shear rate to identify the existence of melt fracture. Because a discontinuity observes in the plot as the melt fracture occur.

As mentioned above, detecting melt fracture phenomenon with capillary rheometer is another benefit using a capillary rheometry. This phenomenon also can be detected with pressure fluctuations in pressure-time plot as shown in Figure 4.13 [57].

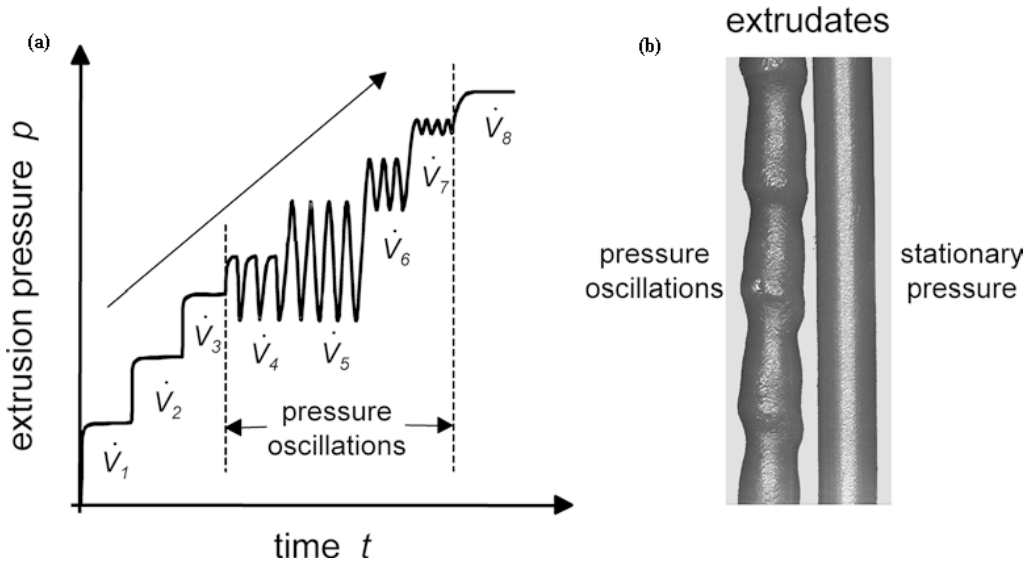

Figure 4.13: Pressure fluctuations indicate melt fracture in HDPE.

Figure 4.13(a) shows typical time dependence of the extrusion pressure of a high molecular weight HDPE melt for a stepwise increase of the flow rate and (b) shows shape of extrudate in the stationary regime of pressure (left) and in the regime of pressure oscillations (right)

4.2.7.1. Wall Slip Measurement

When slip occurs the velocity is not zero at the interface, and the shear rate in the above equation is only a "nominal shear rate" rather than the true shear rate in the melt. Consequently, the true shear rate and the shear stres in the melt are reduıced due to the lessened work required to generate flow when slip is occuring. Figure 4.14 shows slip at the wall as it occurs in a sliding plate rheometer, where V and Vs are the moving plate velocity and the slip velocity respectively [58].

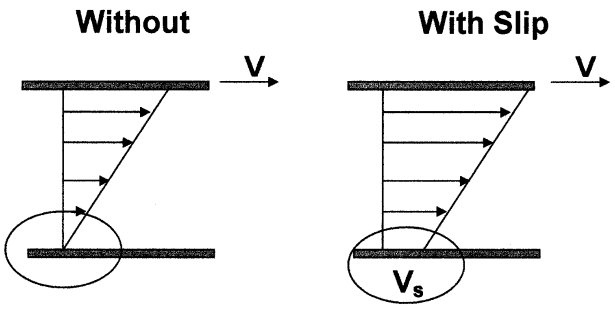

Figure 4.14: Slip at the wall in a sliding plate rheometer.

4.2.7.2. Mooney method

Firstly, in 1931, Money proposed to determine wall slip velocity by using capillary rheometery data. Slip flow can be modelled by the addition of a slip flow velocity to the shear flow velocity. In this case total volumetric flow rate is;

$$Q_{total} = Q_{shear} + Q_{slip}$$

Q_{slip} is given in Equation 4.10.

$$Q_{slip} = \mathrm{V_s}\pi R^2 \qquad \textbf{(4.10)}$$

Where $\mathrm{V_s}$ is the slip velocity of fluid.

As mentioned before, shear viscosity is the ratio of shear stress to shear rate and according to the power law shear viscosity is given in Equation 4.11.

$$\eta = k\dot{\gamma}^{n-1} \qquad \textbf{(4.11)}$$

and true wall shear rate is given in Equation 4.12.

$$\dot{\gamma}_w = \left[\frac{3n+1}{4n}\right]\frac{4Q}{\pi R^3} \qquad \textbf{(4.12)}$$

Using these equations, total volumetric flow rate is given Equation 4.13.

$$Q_{total} = \left[\frac{n\pi R^3}{3n+1}\right]\left[\frac{\tau_w}{k}\right]^{1/n} + v_s \pi R^2 \qquad \textbf{(4.13)}$$

This equation can be rewriten as Equation 4.14.

$$\frac{4Q_{total}}{\pi R^3} = \left[\frac{4n}{3n+1}\right]\left[\frac{\tau_w}{k}\right]^{1/n} + \frac{4v_s}{R} \qquad \textbf{(4.14)}$$

Second term in the above, $\left[\frac{4n}{3n+1}\right]\left[\frac{\tau_w}{k}\right]^{1/n}$, is shear rate value at the wall slip and showed $\dot{\gamma}_{a\infty}$. First term is equal to the apparent shear rate at the given shear stress. Shortly, Equation 4.15 is used to determine wall slip effect.

$$\dot{\gamma}_a = \dot{\gamma}_{a\infty} + 4v_s \frac{1}{R} \qquad \textbf{(4.15)}$$

Money determined wall slip effects on the shear viscosity by using capillaries with constant L/R but different R. For a given wall shear stress, a plot of apparent shear rate values versus the reciprocal of the die radius will give v_s and $\dot{\gamma}_{a\infty}$.

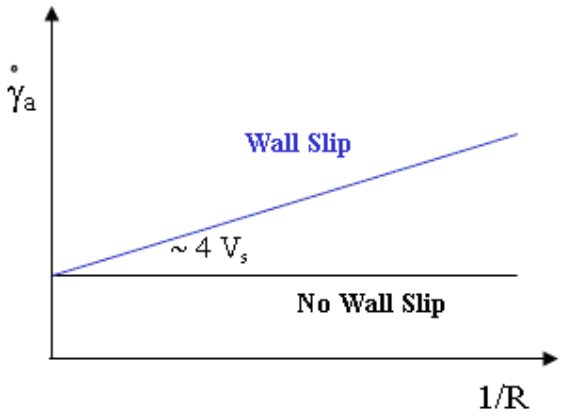

Figure 4.15: Determine wall slip velocity

4.2.8. Pressure -Viscosity Relationship

Experimental investigations into the effect of pressure on the shear viscosity of polymer melts were initiated in the late 1950s by Maxwell and Jung [59]. They

studied on the effect of hydrostatic pressure on the apparent viscosity of high molecular weight polyethylene and polystyrene.

A more comprehensive study was undertaken later by Westover, who was also interested in the effect of pressure on the rheology of polyethylene [60]. He developed a capillary rheometer for this aim. Moreover, Mackley (1995) defined a capillary instrument known as a "multi-pass rheometer" to determine pressure-viscosity relationship [61]. This rheometer consisted of two servo hydraulically controlled pistons. In 1996, Mackley and Spilleler used this instrument to study the pressure dependent rheological behavior of linear low density polyethylene [62]. They investigated that both the apparent viscosity and viscoelastic values increase with tested pressure. Another work has been done by Binding, Couch, and Walters in 1998 [63]. They studied on five polymer melts, high and low density polyethylene, polypropylene, polymethylmethacrylate and polystyrene above 70 MPa using a modified capillary rheometer.

In addition this work, Tomas Sedlacek, Martin Zatloukal, Petr Filip, Antal Boldizar, and Petr Saha studied on the effect of pressure on some polymers for injection molding process by using modified capillary rheometer as seen in Figure 4.16 [64].

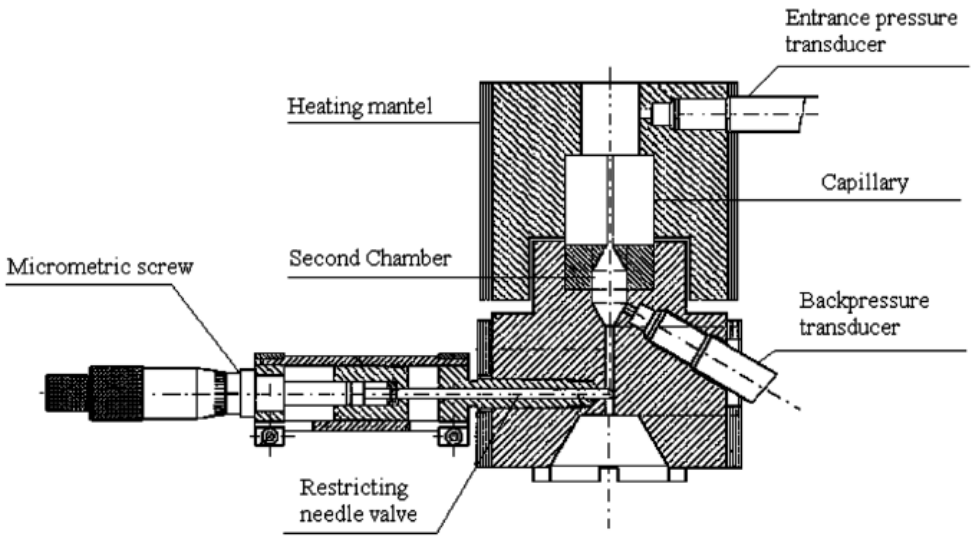

Figure 4.16: Scheme of modified capillary rheometer with a back pressure device.

Here, a second chamber was used to raise polymer melt's pressure.

4.2.9. Die Swell Measurement

As mentioned before, polymer melts show elastic behaviour and consequence of elasticity die swell occurs in melt flow. Many study have been done to explain the origin of die swell phenomenon of polymer fluids. Forexample, Sombatsompop and Dangtungee showed that die swell depend on using die in the capillary rheometer [65]. They researched effect of die design on flow visualization and die swell of NR in a capillary rheometer. For this aim, they designed a type of capillary rheometer as seen in Figure 4.17.

This rheometer has two different dies which one being located at the bottom of the barrel and the other being 35 mm above. They only changed design of Die #2 and a small pressure hole was loceted between the two dies to measure the pressure drop occuring between two dies. They used a colored layer technique to determine the flow patterns in the barrel.

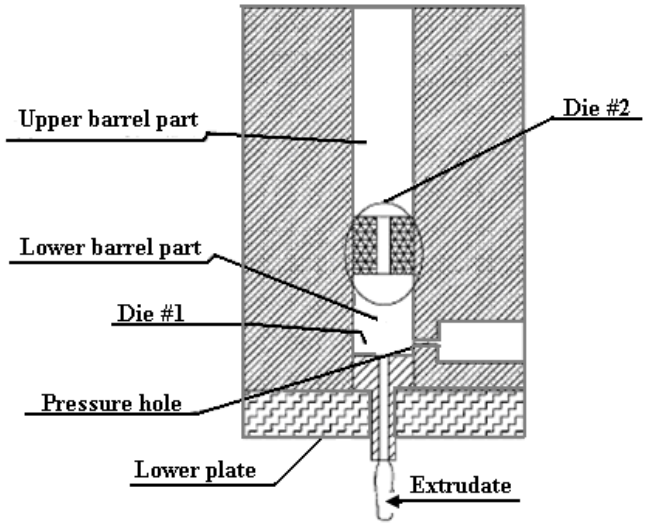

Figure 4.17: Scheme of modified capillary rheometer for die swell measurement.

Consequently, the flows in the upper barrel were found to change with piston displacement but the flows in the lower barrel was dependent not only on the piston displacement, but also on the die design and die swell was found to relate with the flows developed inside the barrel.

In addition Sombatsompop and Intawong also compared with swell ratio of PS in a capillary rheometer and a single screw extruder [66]. They found that the apparent wall shear stress of the PS melt produced from the single screw extruder was higher

than that from the capillary rheometer. At the same time for a given wall shear rate, the extrudate swell ratios from the capillary rheometer and the single screw extruder machines were different, that of the extruder being approximately 20–25% higher. According to the this result the extrudate swell was dominated by the shear stress applied to the polymer melt during the flow.

Also there have been few studies on the melt flow properties of PP and branched polymers, such as low density polyethylene (LDPE) blends, especially on the elastic behaviour of the melts. One of them is Liang and Ness's study. They researched the die swell behaviour of the blend melts and their affecting factors by using a capillary rheometer [67]. They found that the die swell ratio of the blends decreased approximately linearly with increasing temperature and the die L/D ratio and reached a maximum at weight percentage content of PP equal to the twenty.

5. EQUATIONS for SHEAR VISCOSITY MEASUREMENT

Some assumptions are used to derive the viscosity with capillary rheometer as follows;

1. Fully developed, steady, isothermal and laminar flow.
2. The gravitational force is negligible.
3. The fluid velocity is zero at the wall.
4. The fluid is incompressible with viscosity independent of pressure.
5. Entrance and exit effects are ignored.
6. The melt is incompressible.

5.1. Velocity profile inside the tube

When the pressure drives a fluid through a channel, the velocity is maximum at the center. Shear rate and shear stress are maximum at the wall and zero in the center of the flow. This mention was first observed by Hagen.

Parabolic velocity distribution for capillary flow can be find by using these assumptions (Equation 5.1-5.2);

$$v_x = v_x(r), v_\theta = 0 \text{ and } v_r = 0 \quad \textbf{(5.1)}$$

$$v_x(r) = 2v_{ort}\left[1-\left(\frac{r}{R}\right)^2\right] \quad \textbf{(5.2)}$$

Where v_{ort} is the average velocity of the fluid and R is the radius of the capillary. Average velocity can be defined in Equation 5.3.

$$v_{ort} = \frac{Q}{\pi R^2} \quad \textbf{(5.3)}$$

Therefore, shear rate can be calculated by differantiating the velocity profile, Equation 5.4.

$$\dot{\gamma}_a = \left.\frac{dv}{dr}\right|_{r=R} = \frac{4Q}{\pi R^3} = \frac{8v_{ort}}{D} \qquad \textbf{(5.4)}$$

Where $\dot{\gamma}_a$ is the apparent or Newtonian shear rate at the capillary wall.

On the other hand, the wall shear stress (τ_w) can be easily calculated by taking a force balance across the die as given in Equation 5.5.

$\Delta P \pi R^2 = \tau_w 2\pi RL$ and

$$\tau_w = \frac{\Delta P_c .R}{2L} = \frac{\Delta P_c D}{4L} \qquad \textbf{(5.5)}$$

Where L is length of the die and ΔP_c is the pressure drop across the capillary. Thus we have the shear rate and the shear stress at the capillary wall. Therefore, we can calculate viscosity from the Q and ΔP values, Equation 5.6.

$$\eta_{ap} = \frac{\tau_w}{\dot{\gamma}_a} = \frac{\pi .R^4 .\Delta P}{8.Q.L} \qquad \textbf{(5.6)}$$

Where η_{ap} is the apparent viscosity.

5.2. Used Corrections

If the capillary rheometer is used to compare different polymers, it is not necessary to apply the various correction procedures. However, if one wants to know the absolute values of the viscosity, it is important to apply the various correction factors. The most important corrections are Rabinowitsch and Bagley correction.

5.2.1. Rabinowitch Correction

The steady simple shear flow is controllable because the velocity profile depends only on the geometry and motion of the plates. However, fully developed flow in a capillary die isn't completely controllable because velocity profile can be influenced

from the material properties. Therefore, the equaitons used to calculate the apparent viscosity are not suitable for polymer melts. To determine shear rate values of polymer melt, a correction has been developed by Rabinowich using the slope of the shear stress versus shear rate curve.

n is power law index which is calculated from the slope of a log-log plot of the τ_w versus $\dot{\gamma}_a$, Equation 5.7.

$$n = \frac{d\log(\tau_w)}{d\log(\dot{\gamma}_a)} \tag{5.7}$$

Therefore, the true wall shear rate is given in Equation 5.8.

$$\dot{\gamma}_w = \dot{\gamma}_a \left(\frac{3n+1}{4n} \right) \tag{5.8}$$

Schümmer developed a simple approximate method to correct the shear rate. It uses the idea that the true and apparent shear rates must equal one another near the capillary wall. It turns out that this occurs at nearly the same point, $r_c^* = r/R = 0.83$, for a wide range of fluids.

Thus the apparent viscosity equals the true viscosity evaluated as given in Equation 5.9.

$$\dot{\gamma}_w = 0.83\dot{\gamma}_a \tag{5.9}$$

If this approximation is used, viscosity error will be less than 2% for 0.2< n <1.3 [20].

5.2.2. Bagley Correction

In capillary rheometer, flow curve is determined by some parameters such as geometry of the capillary, volumetric flow rate and pressure drop in the die. The volumetric flow rate, Q, can be found directly by using piston speed however determination of pressure drop is not easy because of entrance and exit effects. Figure 5.1 shows how pressure change during the test.

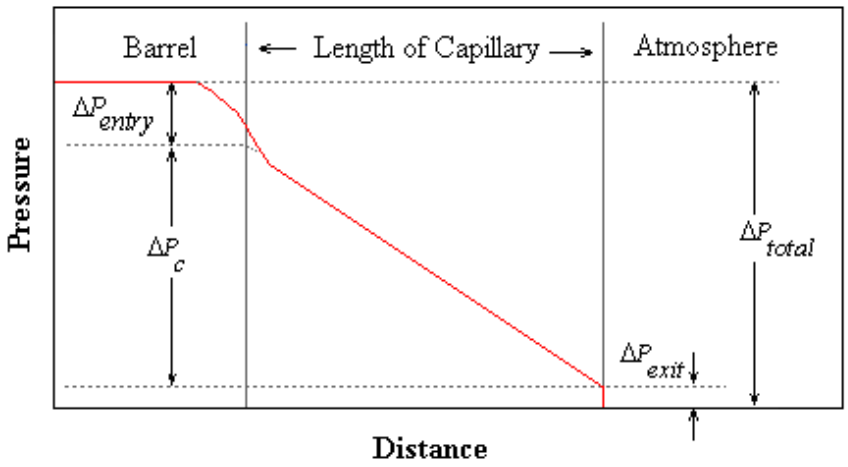

Figure 5.1: Pressure changing in capillar rheometer

Here ΔP_{total} is total pressure drop, measured with pressure transducer. ΔP_{exit} is pressure drop at the capillary exit, ΔP_c is pressure drop along the capillary lenght and ΔP_{entry} is pressure drop at the capillary entrance.

The Bagley correction is used to eliminate pressure differences. This method requires making multiple measurements using dies of the same diameter and different lengths. In this case, the entrance and exit effects will be the same for each die. Therefore the total measured pressure drop, ΔP_{total} ,can be determined as a function of die length.

To apply this correction;

1. The measured pressures are plotted against the L/D of the die for each apparent shear rate as shown in Figure 5.2.

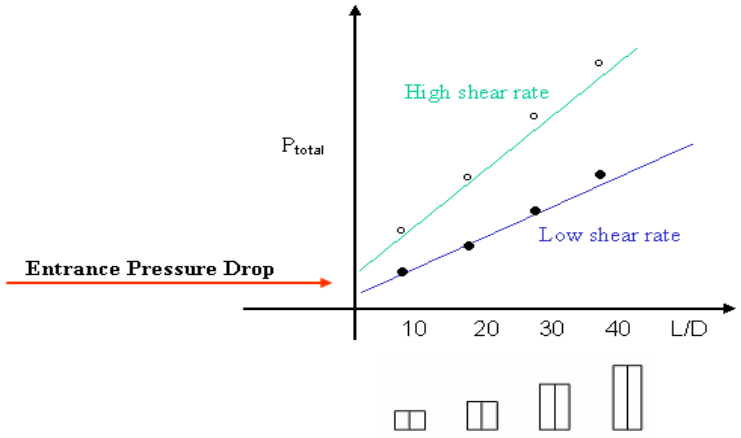

Figure 5.2: Bagley plot

2. Total pressure drop at the exit and entrance area, ΔP_e, is determined by extrapolating back to L/D =0.

3. ΔP_e values subtract from the total pressure drop to determine pressure drop in the die.

Finaly, shear stress is determined from the Equation 5.5 and non- Newtonian shear viscosity is given in Equation 5.10.

$$\eta = \frac{\tau_w}{\dot{\gamma}} \tag{5.10}$$

5.2.2.1. Possible problems in Bagley Correction

Sometimes Bagley correction can't used to determine shear viscosity because linear extrapolation can give physically impossible results as seen in Figure 5.3. This situation can be occur at high L/D ratios Figure 5.3(a) because of wall slip, viscous heating, compressability or at small L/D ratio as given in Figure 5.3(b) [68].

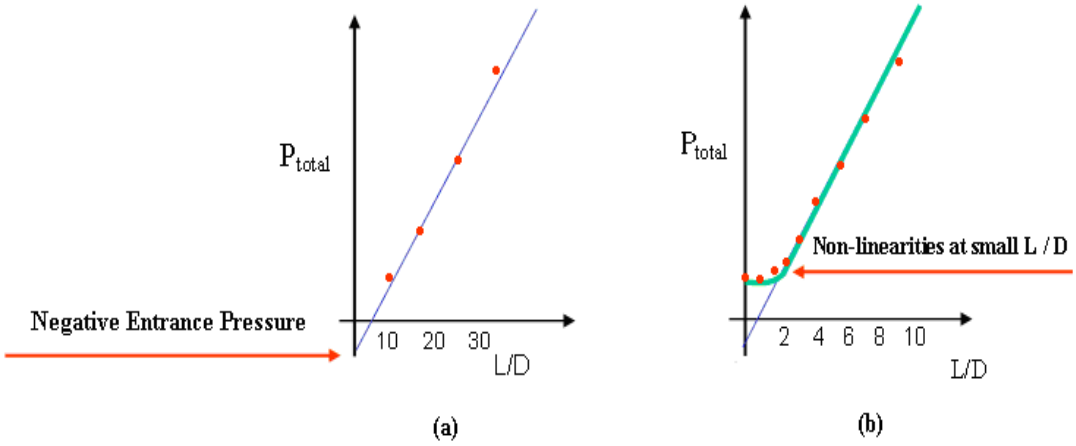

Figure 5.3: Problems in Bagley correction.

In many applications, orifice die can be used to prevent this non-linearities, shown in Figure 5.4. Therefore, pressure drop can be determined free of problems.

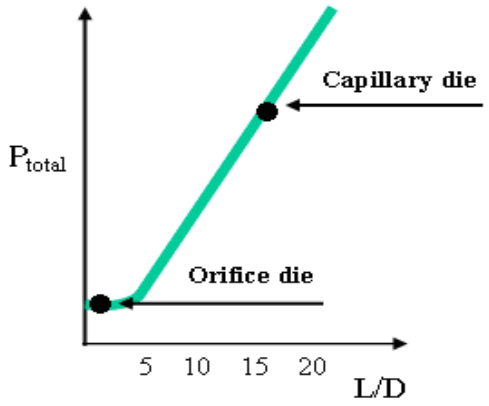

Figure 5.4: Orifice die method.

6. CAPILLARY RHEOMETER DESIGN

As mentioned before, constructing a constant shear rate capillary rheometer capable of measuring rheological properties such as shear viscosity which is the first objective of this study. In this chapter, parts of capillary rheometer were defined shortly.

6.1. Die

Die is the most part of capillary rheometer so die selection should be make carefully. In this study, capillary dies with flat inlet angles are used as recommended in ASTM 3835-96 [69].

6.1.1. Die Material

According to the referance standard, die material should have some properties such as high wear and corrosion resistance and high service temperature. The most generally used capillary die materials are hardened steel, tungsten carbide, stellite and hastelloy.

For this study, selected die material has

- High wear resistance
- High compressive strength
- Very good hardening properties
- Good toughness
- Very good dimensional stability on heat treatment

6.1.2. Die Size

Die sizes should be selected according to the following criterias;

- Desired range of shear rates
- Tested filled and non-uniform materials
- Used different tests such as wall slip or Bagley correction

- Tested low viscosity fluids.

ASTM D 3835-96 recommended following criterias for determining die size;

- Dies should have a flat inlet angle.
- Die length to diameter ratio of the capillary shall normally be between 15 and 40 but for Bagley Plot, standard recommend dies at least one L/D ratio should be less than 10 and at least one should be greater than 16.

Die diameter is important factor to determine the shear rate values because shear rate is a function of the radius cubed so that a 1% error in the radius will result in a 3% error in the shear rate determination. Therefore, die diameter should be provide some criterias such as surface finishing and suitable tolerance values. According to the ASTM D 3835-96, the capillary dies shall have a smooth straight bore that is held to within ± 0.00762mm in diameter and shall be held to within ± 0.025mm in length.

As seen in Table 6.1, dies used commonly have diameters in the range of 0.5 to 3mm.

Tablo 6.1: Die diameters.

Company	Model	Die Diameter
Malvern	RH7-D&RH10-D [70]	0.5 to 3mm
Celsum	Eta 2100 [71]	1mm
Goettfert	Rheo-Tester 1000 [72]	1mm
Haake	RheoCap S20 [73]	0.5, 1 and 2mm

Finishing is another important parameter. Literature indicates that the slip behaviour of polymer melts can be significantly affected by the finish of the die [74]. According to the ASTM D 3835-96, the capillary bore shall be finished about 12rms.

6.2. Piston

6.2.1. Piston Lenght

To determine maximum load applied to a piston or column, first buckling analysis can be used. Figure 6.1 gives flow diagram to use buckling analysis [75].

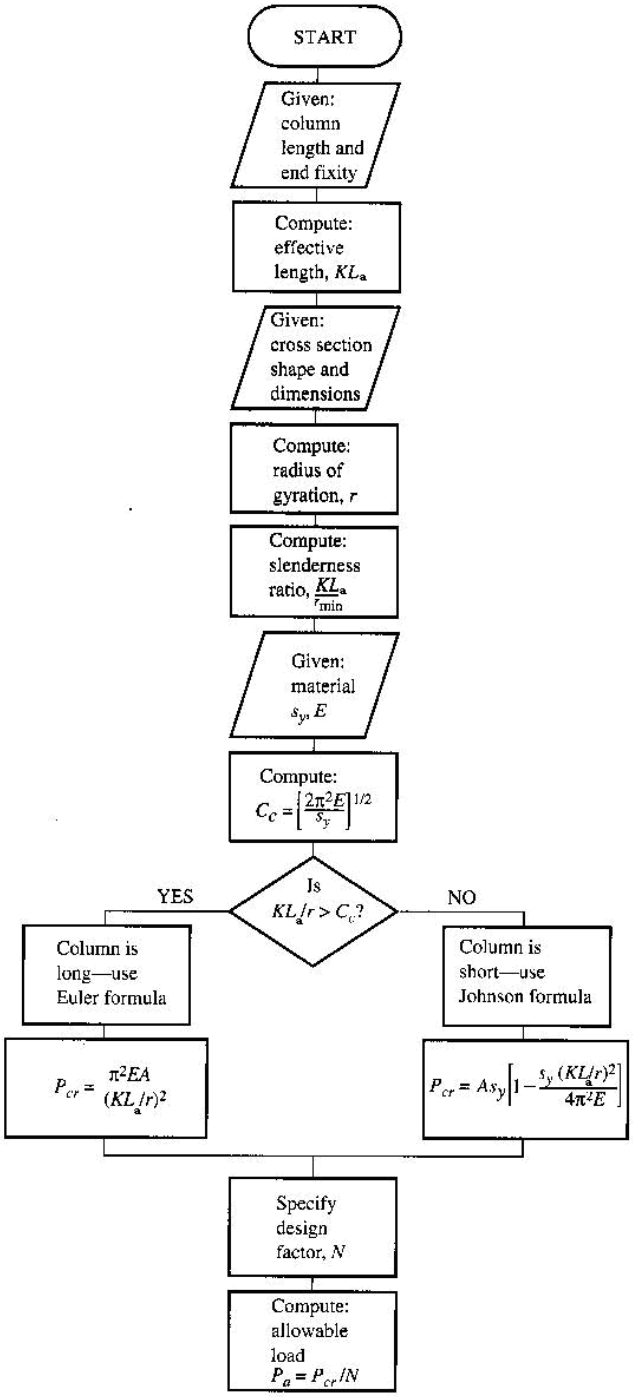

Figure 6.1: Analysis of a straight centrally loaded piston.

According to Figure 6.1,

- Effective piston length (L_e) can be calculated from Equation 6.1.

$$L_e = K.L_a \quad \textbf{(6.1)}$$

Where L_a is actual length of the column between supports and K is constant dependent on the end fixity. Figure 6.2 shows end fixity coefficients of some structures. Here the first values of K are theoretical values and the second values take into account the expected fixity of the piston ends in real, practical structures [75].

K is selected 0.65 in this study because of similarity to design.

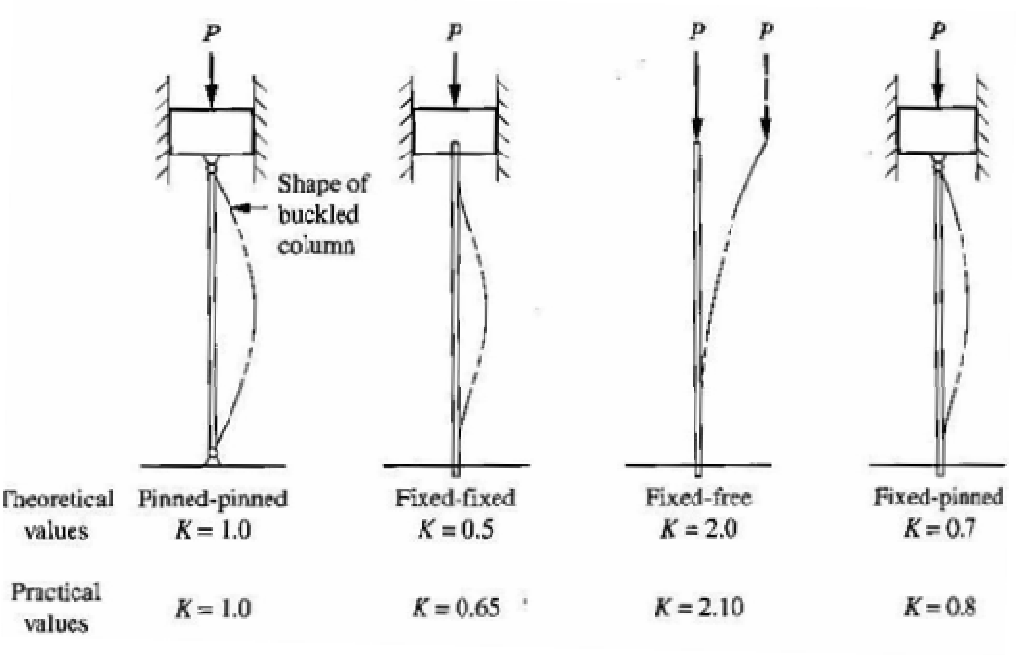

Figure 6.2: End fixity coefficients of some structures.

- Radius of Gyration (r) can be calculated from Equation 6.2.

$$r = \sqrt{\frac{I}{A}} = \frac{D_{piston}}{4} \quad \textbf{(6.2)}$$

Where I is the moment of inertia of the cross section and for circular area it is find from Equation 6.3.

$$I = \frac{\pi D_{piston}^4}{64} \quad \textbf{(6.3)}$$

- Slenderness Ratio can be calculated from Equation 6.4.

$$\text{Slenderness ratio} = \frac{L_e}{r_{min}} = \frac{KL_a}{r_{min}} \quad \textbf{(6.4)}$$

The slenderness ratio is the ratio of the effective length of the column to its least radius of gyration.

There are two methods used for analyzing centrally loaded columns. First is the Euler Formula for long, selender columns and other is J.B Johnson Formula for short columns. The choice of which method to use depends on the column constant.

- Column Constant (C_c) can be calculated from Equation 6.5.

$$C_c = \sqrt{\frac{2\pi^2 E}{S_y}} \quad \textbf{(6.5)}$$

Where E is modulus of elasticity of the material of the column and S_y is yield strength of the material.

Then the value of column constant is computed, it is compared with slenderness ratio. If the slenderness ratio is greater than column constant, the column is called long and in this case, Euler formula is used. However, if the slenderness ratio is less than column constant, the column is called short and in this case, J. B Johnson formula is used.

6.2.1.1. Euler Formula

Euler formula is used for long column analysis and given in Equation 6.6.

$$P_{cr} = \frac{\pi^2 EA}{\left(\frac{KL_a}{R}\right)^2}$$

(6.6)

This equation gives the critical load (P_{cr}) at which the column would begin to buckle. As seen in Equation 6.6, the buckling load is dependent on the geometry of the column and the stiffness of the material represented by the modulus of elasticity.

6.2.1.2. J.B Johnson Formula

J.B Johnson formula is used to short piston. This formula is given in Equation 6.7.

$$P_{cr} = AS_y \left[1 - \frac{S_y \left(\frac{KL_a}{r} \right)^2}{4\pi^2 E} \right] \quad \textbf{(6.7)}$$

6.2.1.3. Allowable Load (Pa)

The objective of piston analysis and design is to ensure that the load applied to a column is safe, below the critical buckling load. Equation 6.11 is used to determine allowable load but the actual load (P) must be less than this value [75].

$$P_a = \frac{P_{cr}}{N} \quad \textbf{(6.8)}$$

Here N is design factor, P_{cr} is critical buckling load and P_a is allowable load. Design factor is equal to 3 for typical machine design applications. Table 6.1 gives calculated allowed load values for a material which has 300MPa yield strength and 207GPa modulus of elasticity using different barrel diameters.

Table 6.1: Allowed piston load for a material having Sy=300MPa and E=207GPa.

Barrel Diameter (D_b ,mm)	**Piston Diameter** (D_p ,mm)	**Allowed Load (kN) for the Lenght of Piston (mm) is;**		
		L_p =300 mm	L_p =400 mm	L_p =500 mm
15	14	13,6	12,4	10,6
	13	11,5	10,1	8,4
	12	9,6	8,2	6,5
11	10	6,1	4,7	
9,55	9	4,6		

As seen in Table 6.1, allowed piston load decreases as the piston lenght is incresed and barrel diameter is decreased. In this study, the tensile testing machine used has apply max. 20kN piston load so allowed piston loads in Table 6.1 are too small to extrudate high viscous material. To solve this problem, a different material which has 1280Mpa yield strength is equal to 1280MPa and 207Gpa was selected. Table 6.2 shows results for this material.

Tablo 6.2: Allowed piston loads for selectived piston material.

Barrel Diameter (D_b ,mm)	**Piston Diameter** (D_p ,mm)	**Allowed Load (kN) for the Lenght of Piston (mm) is;**				
		L_p=200	L_p=250	L_p=275	L_p=300	L_p=350
15	14			32.5	23.9	20.8
	13	42.1	33.9	24.5	24.2	17.9
	12	33.7	25.5	20.9	17.9	
11	10	19.0	13.5	10	8.4	
9.55	9	12.5	8.0	6.8	5.5	

Second material having is Sy =1280MPa and E =207Gpa stronger than first material because of high yield strength value. Consequently, if barrel diameter is equal to the 15mm, max piston load is enough for the tensile machine capacity.

6.2.2. Piston Size

The piston is divided into two parts, piston body and piston tip, as seen in Figure 6.5.

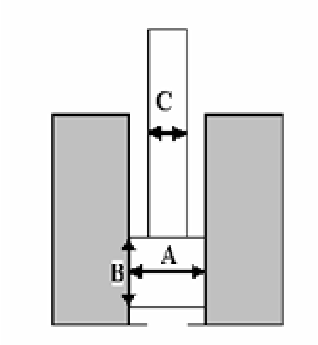

Figure 6.5: Piston sizes

According to the ASTM D 3835-96

- The land of the piston, represented with A, shall be 0.0254 ± 0.007mm smaller in diameter than the barrel. So, max. and min. values of A are;

$$A_{\max} = D_{barrel} - (0.0254 - 0.007)$$

$$A_{\min} = D_{barrel} - (0.0254 + 0.007)$$

- The land of the piston, represented B, shall be at least 6.35 ± 0.13mm in length. So, max and min. values of B are;

$$B_{\max} = 6.35 + 0.13 = 6.48\text{mm}$$

$$B_{\min} = 6.35 - 0.13 = 6.22\text{mm}$$

- Above the land, represented C, the piston shall be relieved at least 0.25mm less than the barrel diameter. So, max and min. values of C is;

$$\mathrm{C}_{\max} = 14.75\text{mm}$$

Consequently, if barrel diameter is selected 15mm, A should be between 14.96-14.98mm and C is 14.75mm.

These tolerances are necessary for piston-barrel sealing.

6.3. Barrel

6.3.1. Barrel Material

Generally, nitrided steel is used to provide hardness and toughness for barrel material. However, barrels from the other materials may be required where the samples adhere to the steel making cleaning difficult such as Polyether sulfone (PES) and Polyetheretherketone (PEEK) , where a sterile environment is required such as pharmaceutical and food, or where the sample may corrode the steel or degrade to produce corrosive products [76].

Barrel and piston material selected in this study have;

- Good resistance to abrasion at both low and high temperatures
- High level of toughness and ductility
- Uniform and high level of machinability and polishability
- Good high-temperature strength and resistance to thermal fatigue
- Excellent through-hardening properties

6.3.2. Barrel Size

According to the ASTM D 3835-96, the barrel shall have a smooth, straight bore between 6.35 and 19mm in diameter". The larger barrel is an advantage to generate higher shear rates but the smaller barrel requires less time for the test sample to reach thermal equilibrium. In general, a sample size of 10-50g is used in many commercial instruments. The standard 15mm diameter barrel holds about 50cm³ of sample. According to the Malvern Instrument, a barrel diameter of 15mm offers a good compromise [76]. Therefore, barrel diameter of 15mm is selected for this study.

As seen in Table 6.3, commercial capillary rheometers are available with barrels in the range of 9.5 to 24mm in diameter.

Tablo 6.3: Barrel size of some commercial capillary rheometers.

Company	Model	Barrel Diameter (mm)	Barrel Length (mm)
Haake	RheoCap S20[77]	9.55; 12 and 15	197
Malvern	RH7-D&RH10-D[70]	9.5; 15; 19 and 24	280
Celsum	Eta 2100[71]	20	320
Göttfert	Rheo-Tester 1000[72]	9.55 and 12	200
Ceast	SmartRheo1000/2000[78]	9.5; 10; 12 and 15	160 and 290

6.3.3. Maximum Pressure in the barrel

Using tensile machine can provide max. 20kN, in this case, maximum pressure in the barrel is equal to the 1132 bar as shown below.

$$\mathrm{F}_{\max} = 20\mathrm{kN} = 2\times10^{4}\,\mathrm{N}$$

$$P_{\max} = \frac{F_{\max}}{A_{\mathrm{barrel}}} = \frac{2\times10^{4}\,\mathrm{N}}{176.6\times10^{-6}\,\mathrm{m}^{2}} = 1132\times10^{5}\,\mathrm{Pa} = 1132\mathrm{Bar}$$

6.3.4. Minimum wall thickness of barrel

Minimum wall thickness must be calculate as given below;

$$S_{\min} = \frac{D_{barrel}\times P_{\max}}{2\times\sigma} = \frac{15(\mathrm{mm})\times113.2(\mathrm{MPa})}{2\times1820(\mathrm{MPa})} \cong 0.5\mathrm{mm}$$

Where σ is tensile strength value of barrel material and $S_{\min}$ is minimum wall thickness of barrel. Therefore safe wall thickness is find using $S_{\min}$ and N as below;

$$S = S_{\min}\times\mathrm{N} = 0.5\times3 = 1.5\mathrm{mm}$$

where N is design factor as mentioned before.

6.4. Operation Control Systems

Operation control systems can be divided into two seperate systems, these being pressure and temperature control systems.

6.4.1. Pressure Measurement

As mentioned before to calculate shear stress values, pressure drop along the die must be know, and then pressure or force transducers must be used. Pressure transducers or transmitters are generally used for high-accuracy measurements while force transducers are generally used in quality control labs. These transducers will not come in contact with corrosive or very high temperature samples but piston friction can be significant as material flow along barrel. Therefore, a pressure transmitte was selected for this study and it has following properties;

- Installation for media temperature up to 400 °C
- Pressure range is 0-2000bar
- Accuracy is ±0.5% - up to 50 bar ±1%
- Repeatability is ±0.1%- up to 50 bar ±0.2%
- Max. diaphragm temperature is 400ºC

Pressure range was selected high because this rheometer is used for research and development studies so some very highly filled materials can be tested. In this case, pressure values are higher than pure polyolefines.

6.4.2. Temperature Measurement

Temperature control plays an important role because viscosity is highly dependent of temperature so temperature must be carefully controlled during the. In this study, system is electrically heated with two heater jackets around the reservoir and temperature is measured by RTD.

7. EXPERIMENTAL PART

Before running capillary rheometer, test temperature and piston speed must be determined.

7.1. Set Up Parameters

7.1.1. Temperature

Temperature is one of the most important parameters to be specified, as viscosity is a strong function of temperature. The temperature must be high enough to melt the sample completely and low enough that the saple will not degrade during the test. Once a temperature is chosen, a thermal degradation study should be performed to determine the maximum residence time of the material in the rheometer. Meaningful test temperatures can often be found in ASTM specification. Standard testing temperatures suggested by ASTM D 3835 are given in Table 7.1.

Table 7.1: Standart testing temperature suggected by ASTM D 3835.

	Typical Test Temperature (ºC)
Acetals	190
Acrylics	230
Acrylonitrile-butadine-styrene	200
Cellulose esters	190
Nylon	235 to 275
Polychlorotrifluoroethylene	265
Polyethylene	190
Polycarbonate	300
Polypropylene	230
Polystyrene	190 to 230
Poly(vinyl chloride)	170 to 205
Poly(butylene terephthalate)	250
Thermoplastic Elastomer (TES) Unsaturated	150 to 210
Thermoplastic Elastomer (TES) Saturated	180 to 260

7.1.2. Shear Range Selection

A typical test range for an average extrusion process might be from 20 to 2000 s^{-1}, whereas testing for an injection molding process might be more relevant across a range of 200-20,000 s^{-1} [21]. In this study, selected test materials are used in extrusion processing so shear rate values should be suitable for this process.

Apparent shear rate values can be determined from Equation 7.1.

$$\dot{\gamma}_a = \frac{4V_p R_b^{\,2}}{R^3} \qquad \textbf{(7.1)}$$

Here, R_b is barrel radius, R is die radius and V_P is piston speed.

The piston speed is linear function of the shear rate that is strongly affected by the geometry of both the barrel and die.

7.1.3. Min. and max. piston speeds

Min. and max. piston speeds can be calculated from Equation 7.2.

$$V_p = \frac{\dot{\gamma}_a R_d^{\,3}}{4R_b^{\,2}} \qquad \textbf{(7.2)}$$

For R_b = 7.5mm ; R_d = 0.5mm and

shear rate range (for extrusion process) = 20-2,000 s^{-1},

Min. piston speed = 0.67 mm/min

Max. piston speed = 66.67 mm/min

7.2. Test Material and Procedure

In this study, the high density polyethylene granules are tested at 190℃ according to the testing procedure. The test prosedure is given below.

1. Barrel was filled with HDPE granules and heated until the desired temperature.
2. Molten polymer flown through the die at constant piston speed which was between 0.66-18.3 mm/min.
3. Pressure was measured by a pressure transducer attached enter the die.

The properties of HDPE used are given in Table 7.2..

Table 7.2: Propereties of used HDPE.

Company	Code	Lot	MFI (g/10min) (at 190 °C and with 5kg weigth)	Density (g/cm³)
National Petrochemical Company	NPCBL3	185095	0.89	0.95

7.3. Capillary Rheometers Used For Comparision Test Results

The rheometers produced by Dynisco (Figure 7.1) and Malvern Instruments (Figure 7.2) were used to compare the test results obtained from capillary rheometer designed in the study [79].

Figure 7.1: Dynisco LCR 7000 capillary rheometer

Figure 7.2: Malvern RH 10D capillary rheometer

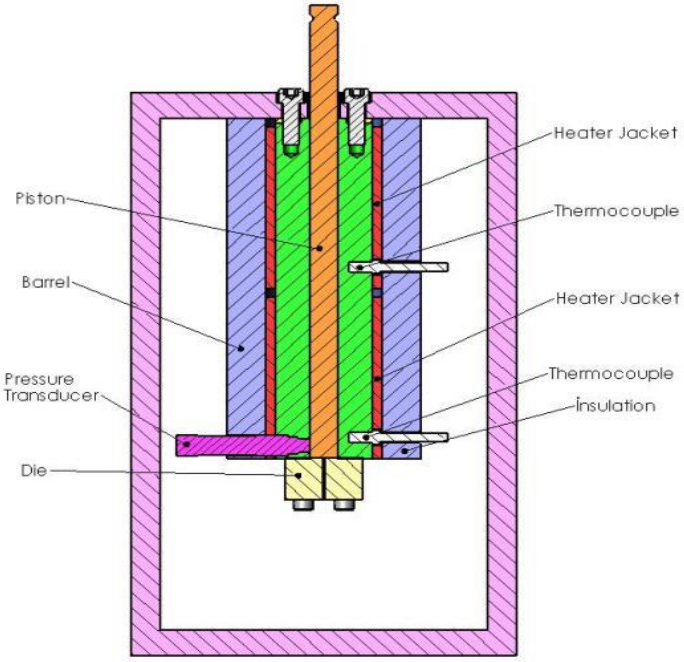

Figure 7.3: Designed capillary rheometer

Some properties of rheometers used are given in Tables 7.3-7.5.

Table 7.3: Dynisco LCR 7000 capillary rheometer.

Barrell	Lenght = 162mm Diameter = 9.55mm
Piston Speed	0,03 to 600 mm/min
Testing Force	5 or 10 kN standard and 15 kN (optional)
Force Measurement	Load cell standard, barrel mounted pressure transducer
Dies	Many L/D ratios available
Temperature Range	up to 430 ºC Standard
Temperature Control	4 zone electric heater
Temperature Sensor	4-wire Platinum RTD
Die Swell Measurement	Laser-Micrometer (optional)

Table 7.4: Malvern RH 10D capillary rheometer.

Barrell	Lenght = 280mm Diameter = 5; 9,5; 19 and 24mm
Drive Speed Maximum	1200mm/min
Pressure Transducer Ranges (PSI)	30000, 20000, 10000, 5000, 1500, and 500
Pressure Transducer Accuracy	Better than 0.5%
Testing Force	100kN
Dies	0.5 to 3mm
Temperature Range	Ambient to 400ºC, 500ºC (option)

Table 7.5: Designed capillary rheometer.

Barrell	Lenght = 200mm Diameter = 15mm
Piston	Lenght = 260mm Diameter = 14mm
Pressure Transducer Ranges (Bar)	0-2000
Pressure Transducer Accuracy	Better than 0.5 %
Maximum Testing Force	20kN
Dies	Diameter = 1mm Lenght = 5, 10, 20, and 25mm
Temperature Range	Ambient to 400ºC
Heating Jacket	Lenght = 90mm Diameter = 50mm Power = 450Watt Voltage = 220V

8. RESULTS OF CAPILLARY RHEOMETRY MEASUREMENTS

Bagley plots were drawn from the designed capillary rheometer results then shear stress was calculated. Finally, results compared with RH 10D and LCR 7000 rheometers.

8.1. Apparent Shear Rate Values

Apparent shear rate values calculated from Equation 7.1 are given in Table 8.1.

Table 8.1: Apparent shear rate values for HDPE.

Plunger Speed (mm/min)	Apparent Shear Rate (1/s)
18.3	549
9.41	282.3
4.83	144.9
2.48	74.4
1.27	38.1
0.66	19.8

8.2. Bagley Plots

During the test, pressure values were recorded to apply the Bagley correction and then shear stress was calculated by using pressure drop along the capillary. Tables 8.2-8.5 show measured pressure values for each L/D ratio and plunger speeds. Bagley plots of HDPE for five different shear rates are given in Figure 8.1.

Table 8.2: Measured pressure values for L/D=5.

	Plunger Speed (mm/min)	Measured Pressure (Bar)
L/D=5	18.3	78
	9.41	62
	4.83	49
	2.48	39
	1.27	30
	0.66	23

Table 8.3: Measured pressure values for L/D=10.

	Plunger Speed (mm/min)	Measured Pressure (Bar)
L/D=10	18.3	118
	9.41	95
	4.83	74
	2.48	62
	1.27	49
	0.66	37

Table 8.4: Measured pressure values for L/D=20.

	Plunger Speed (mm/min)	Measured Pressure (Bar)
L/D=20	18.3	230
	9.41	188
	4.83	153
	2.48	122
	1.27	95
	0.66	75

Table 8.5: Measured pressure values for L/D=25.

	Plunger Speed (mm/min)	Measured Pressure (Bar)
L/D=25	18.3	276
	9.41	226
	4.83	182
	2.48	145
	1.27	115
	0.66	88

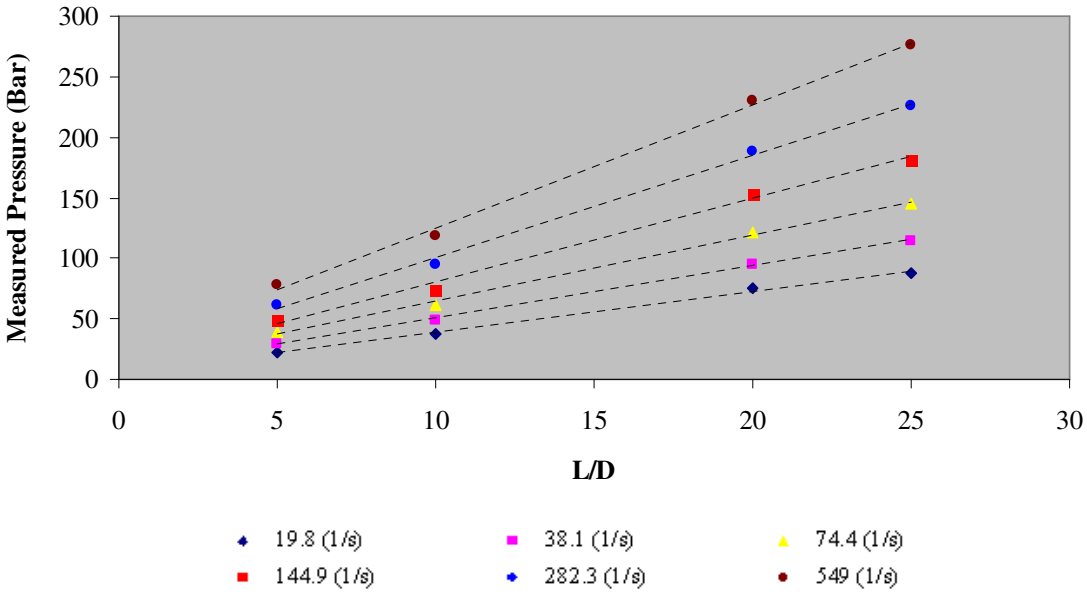

Figure 8.1: Comparing the Bagley plots.

Linear regression analysis results are given in Table 8.6.

Table 8.6: Linear Regression Results.

Shear Rate (1/s)	R^2
19.8	0.995
38.1	0.998
74.4	0.997
144.9	0.994
282.3	0.996
549	0.997

As seen in Figure 8.1, pressure increases with increasing shear rate and L/D ratio. This result is expected because according to Equation 5.5, the pressure drop is correlated to the shear stress and L/D ratio of capillary and according to the Power law, shear stress is depend on shear rate values. Thefore shear stress increase with increasing shear rate. The similar results are given in literature [33, 88].

8.3. Calculating Shear Stress

Shear stress values were calculated with Equation 5.5 and Table 8.6 shows these results.

Table 8.7: Shear stress values for HDPE.

Shear Rate (1/s)	L/D	Measured pressure (Bar) (ΔPtot)	ΔPend (Bar)	Average Shear Stress (Pa)
549	5	78	23.1	255818.8
	10	118		
	20	230		
	25	276		
282.3	5	62	16.45	212028.1
	10	95		
	20	188		
	25	226		
144.9	5	49	11.05	173565.6
	10	77		
	20	153		
	25	184		
74.4	5	39	10.4	136525
	10	62		
	20	122		
	25	145		
38.1	5	30	7.45	108403.1
	10	49		
	20	95		
	25	115		
19.8	5	23	5.35	84271.88
	10	37		
	20	75		
	25	88		

8.4. Comparision of Apparent Shear Viscosity Results for HDPE

Figure 8.2 shows comparision of experimental results which gained from the capillary rheometers used. As can be seen, good agreement between results is obtained.

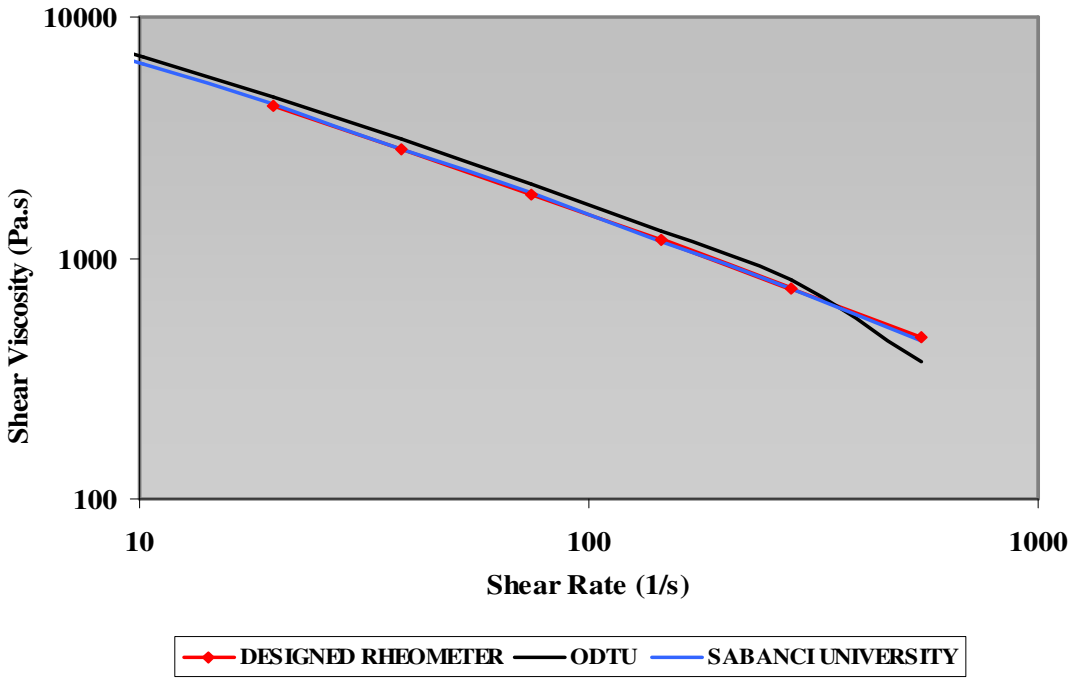

Figure 8.2: Comparison of apparent shear viscosity results.

8.5. Determine Power Law Index

In order to determine true the shear rate, the slope should be find by plotting the $\ln(\tau_w)$ versus the $\ln(\dot{\gamma}_a)$ as shown in Figure 8.3.

As known polyethylene melts, like many other polymeric materials, deviate from ideal Newtonian behavior. The corrected shear viscosity of HDPE ,η , can be calculated using Equation 5.10 which is the shear stress divided by the actual shear rate. Table 8.7 shows shear viscosity data and Figure 8.4 shows flow curve of HDPE.

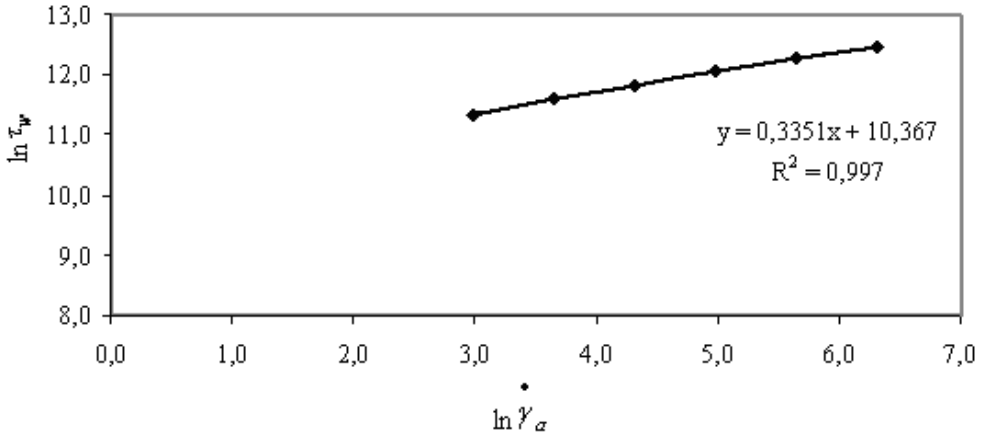

Figure 8.3: Plot of the ln (τ_w) versus ln ($\dot{\gamma}_a$) for HDPE at 190℃.

Table 8.8: Shear viscosity values of HDPE.

	Apparent Shear Rate (1/s)	**Power Law Index (n)**	**Corrected Shear Rate (1/s)**	**Corrected Shear Viscosity (Pa.s)**
HDPE	549	0.33	827.34	309.21
	282.3	0.33	425.43	498.39
	144.9	0.33	218.36	794.84
	74.4	0.33	112.12	1217.66
	38.1	0.33	57.42	1888.01
	19.8	0.33	29.84	2824.26

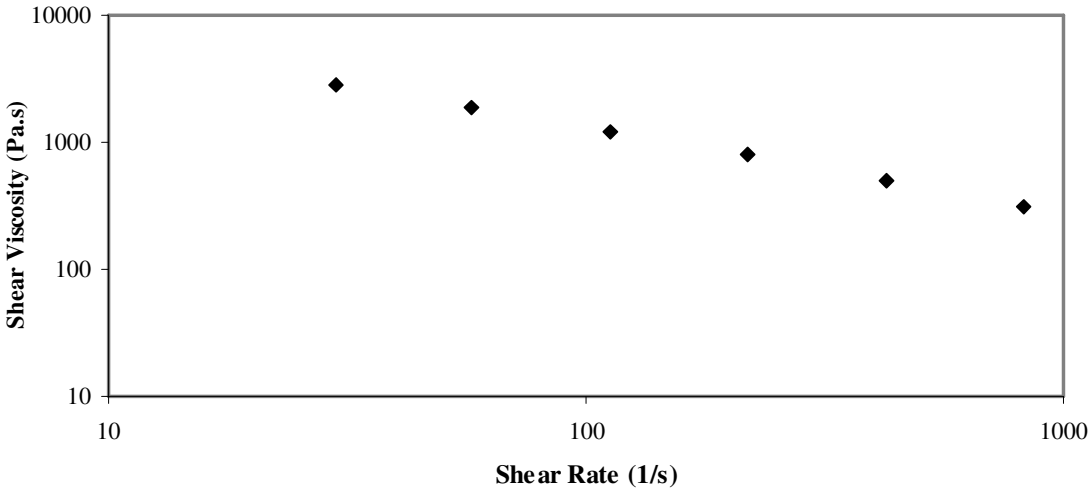

Figure 8.4: Flow curve of HDPE at 190℃.

9. CONCLUSIONS

In this study, a simple capillary rheometer was designed according to the ASTM standards. As a part of the rheometer a tensile testing machine was attached for the push and pull movements. The rheometer was tested with HDPE using three different dies and the results were compared with those of the rheometers which are produced by Malvern and Dynisco Instruments. The operation temperature was adjusted 190°C. The rheometer designed in this study gave the similar results with the commercial rheometers used. As a view of design parameters, the main difference is that requiring force is generated by a tensile testing machine in the rheometer developed in this study. For this reason, the cost for producing it is lower than that of commercial rheometer.

The importance of this study is that a scientific study was done and published about rheometer design due to there is only patent publications in literature. In the future, the data for solving some processing problems such as melt fracture or die swell can be obtained by using capillary rheometer designed and the effects of some parameters such as temperature, pressure and, type and amount of additives on rheological behavior can be determined. So, obtained data can be used for improving the process conditions. Additionally, software can be written to make the calculations easily and a twin bore capillary rheometer can be designed for doing the tests in a short time.

REFERENCES

[1] **Morrison, F.A.,** 2004. What is rheology anyway?, *The Industrial Physicist,* 10(2), pp 29-31.

[2] **Doraiswamy, D.,** 2001. The origins of rheology: a short of historical extrusion, *DuPont Technologies*, Wilmington.

[3] http://www.afns.ualberta.ca/Courses/Nufs403/PDFs/chapter3.pdf , 2007.

[4] **Ferguson J. and Kemblowski Z.,** 1991. Applied Fluid Rheology, *Elsevier Applied Science,* New York.

[5] **Vlachopoulos J.,** 2003. The Role of Rheology in Polymer Extrusion, *New Technologies for Extrusion* C*onference*, Milan, Italy.

[6] www.rheologyschool.com/id46.html, 2007.

[7] **Polyflow user guide**

[8] **Donald G.B. and Dimitris I.C.,** 1998. Polymer Processing Principles and Design, Wiley Interscience Publication, Canada.

[9] **Young G.S.,** 1989. In line viscosity measurement for the gear pump assisted single screw extrusion process. Master Thesis, University of Lowel.

[10] **Baumann, G.F. and Steingiser, S.,** 1963. Rheological measurements on polycarbonate, *J.Polym Sci.,* A1, 3395-3406

[11] **Fox, T.G., Grateh, S., and Loshach, S.,** 1956. Viscosity Relationships for Polymers in Bulk and in Concentrated Solution in Rheology, *Academic Press*, New York

[12] **Kraus, G. And Gruver, J.L.,** 1965. Rheological properties of cis-polybutadine, *J.Appl.Polym. Sci.,***9**, 739-755.

[13] **Porter, R.S. and Johnson, J.F.,** 1963. The effect of molecular weight and distribution on polymer rheology near the entanglement region, *Trans. Soc. Rheol.*, **7**, 241-252

[14] **Cogswel, F.N. and McGowan, J.C.,** 1972. The effect of pressure and temperature upon the viscosities of liquids with special reference to polymeric liquids, *British Polymer Journal*, **4**, 183-198.

[15] **Cogswell, F.N.**, 1973. The influence of pressure on the viscosity of polymer melts, *Plast. Polym*, **14***,* 39-43.

[16] **Sedlacek, T., Zatloukal, M., Filip, P., Boldizar, A., and Saha, P.,** 2004. On the Effect of Pressure on the Shear and Elongational Viscosities of Polymer Melts, *Polym. Eng. Sci*. **44**: 1328–1337.

[17] https://www.hansergardner.com/sample/1-56990-369-7.pdf, 2007.

[18] http://www.mkn.itu.edu.tr/~arana/IML212-N6.pdf, 2007.

[19] **Graessley, W., Glasscock, S.D., and Crawley R. L.,** 1970. Die swell in molten polymers, *Trans. Soc. Rheol*. **14** (4), 519-544.

[20] **Macosko C.W.,** 1994**.** Rheology: Principles, Measurements, and Applications, *Wiley-Vch,* Canada.

[21] **Lobo, H. and Bonilla J.V.,** 2003. Handbook of Plastics Analysis, CRC press.

[22] http://www.dynisco.com/literature/Technical%20Articles/NewApproach.pdf, 2007.

[23] **DeLaney, D.,** 1998. A new Approach to polymer rheology for process and quality control*, Plastics Engineering*, Vol.**54**, Iss.6;p.45(3).

[24] **Fellers, J. and Hansen, M.** 2002. University of Tennessee Knoxville Materials Science and Engineering Department Special Project Professors: Dynamic Stress Rheometer.

[25] www. ciks.cbt.nist.gov/~garbocz/SP946/node14.htm, 2007.

[26] http://lww.kt.dtu.dk/~vigild/2005_03_dyrup/Theory.htm, 2007.

[27] http://www.mat.chalmers.se/kurser/mpm080/lab-rheology.pdf, 2007.

[28] **Mandis, S.L.,** 2004. Rheometers: Which type is right for you?, *Plastic Technology*, **50**, 64-73.

[29] **Green, G.R.M.,** 1997. Laboratory viscometry a review, *Pigment & Resin Technology*, Volume **26**, Number 6, 357-362(6)

[30] **Rides, M. and Allen, C.,** 2006. Slip flow measurement by capillary extrusion rheometry, *Measurement Good Practice Guide,* 90.

[31] http://www.brabender.com/53.0.html, 2007.

[32] **Etamad, S.G.,** 1998. Design and Construction of capillary rheometer, *Iranian Polymer Journa*l, Volume 7 number2.

[33] **Laun, H.M.,** 2004. Capillary rheometry for polymer melts, *Rheol Acta,* **43**, 509-528.

[34] **Goettfert, A.,** A Novel Gas Driven Dual Barrel Capillary Rheometer, *Goettfert*, Germany.

[35] **McAfee, M. and McNally, G.,** 2006. Real-time measurement of melt viscosity in single-screw extrusion, *Transactions of the Institute of Measurement and Control* **28**; 481.

[36] **Fleming, D.J,** 1993. In-line rheometry studies in reactive extrusion. *PhD Thesis*, University of Bradford.

[37] **Padmanabhan, M. and Bhattacharya, M.,** 1994. In-line measurement of rheological properties of polymer melts, *Rheologica Acta,* **33**, 71-87.

[38] **Rauwendaal, C. and Fernandez, F.,** 1985. Experimental study and analysis of a slit die viscometer. *Polymer Engineering and Science*, **25**, 765-71.

[39] **Kalyon D.M., Gokturk, H. and Boz, I.,** 1997. An adjustable gap in-line rheometer, *SPE Antec Technical Papers*, **43**, 2283-2288.

[40] **Covas, A., No´brega, J.M. and Maia, M.,** 2000. Rheological measurements along an extruder with an on-line capillary rheometer, *Polymer Testing,* **19**,165-176.

[41] **Whorlow, R.,** 1992. Rheological Techniques, Ellis Horwood, London.

[42] **Huang, J.C. and Junke, Xu.,** 2003. Thermal degradation of polypropylene in a capillary rheometer, *International Journal of Polymeris Materials*, **52**, 203-209.

[43] www.instrument.com.cn/show/download/download_show.asp?type=4&IMShowID=SH100699&id=6369, 2007.

[44] **Fellers, J.F. and Hansen, M.,** 2002. Measurements Of Melt Viscosities Of Polypropylene with the instron capillary rheometer**,** Mse 494.

[45] **Modigell, M., Hufschmidt, M. and friends.,** 2000. Investigation of wall slippage in suspensions by NMR imaging, *Proceedings XIIIth International Congress on Rheology*, Cambridge, UK.

[46] **Chen, Y., Kalyon, D.M. and Bayramli, E.,** 1992. Wall slip behavior of linear low density polyethylene, *SPE ANTEC Technical Papers,* **38**, pp.1747-1751.

[47] **Ramamurthy, A.V.,** 1986. Wall slip in viscous fluids and Influence of material of construction, *Journal of Rheology*, **30**(2), 337.

[48] **Kalika, D.S., and Denn, M.M.,** 1987. Wall slip and extrudate distortion in linear low density polyethylene, *Journal of Rheology*, **31**(8), 815.

[49] **Georgiou, G., Vlassopoulos, D. And Fyrillias, M.,** 1999, A Mechanism for Extrusion Instabilities in Polymer Melts, *Polymer Engineering and Science*, Vol.**39**, No:12.

[50] **Drda, P. A. and Wang, S. Q.,** 1995. Hydrodynamic Slip: Polymer adsorption and desorption at melt/solid interfaces, *Phys. Rev. Lett,* 75, 2698.

[51] **Sornberger, G., Quantin, J. C., Fajolle, R., Vergnes, B., and Agasant, J. F. J.,** 1987. Experimental study of the sharkskin defect in linear low density polyethylene, *Non-Newtonian Fluid Mech*, **23**, 123-125.

[52] **Ui, J., Ishimaru, Y., Murakami, H., Fukushima, N., and Mori, Y.,** 1964. Study of flow properties of polymer melt with the screw extruder, *SPE Trans,***10**, 295-305.

[53] **Ballenger, T. F., Chen, I., Crowder, J. W., Hagler, C. E., Bogue, D. C., White, J. L.,** 1971. Polymer melt flow instabilities in extrusion investigation

of the mechanism and material and geometric variables, *Trans Soc Rheol,***15**, 195.

[54] Akay, G., 1983. Unstable capillary flow of reinforced polymer melts, *Journal of Non-Newtonian Fluid Mech.,***13**, 309-323.

[55] Fujiyama, M. and Kawasaki, Y., 1991. Rheological properties of PP/HDPE blend melts. I. Capillary flow properties, *Journal of Applied Polymer Science,* **42**, 467-480.

[56] Huang, J.C. and Tao, Z., 2003. Melt Fracture, Melt Viscosities, and Die Swell of Polypropylene Resin in Capillary Flow, *Journal of Applied Polymer Science,* **87,** 1587-1594.

[57] Laun, H., 2004. Capillary rheometry for polymer melts revisited, *Rheologica Acta*, **43,** 509-528.

[58] Smillo, F., 2004. Wall slip and spurt of molten polymer, Ms. Thesis, McGill University, Montreal, Canada.

[59] Maxwell, B. and Jung, A., 1957. Hydrostatic pressure effect on polymer melt viscosity, *Modern Plastics,* **35**, 174-182&276.

[60] Westover, R.F., 1961. Effect of hydrostatic pressure on polyethylene melt rheology*, SPE Trans*. 1, 120.

[61] Mackley, M.R., Marshal, R.T.J. and Smeulders, J.B.A.F., 1995. *Journal of* . *Rheology*, **39**, 1293.

[62] Mackley, M.R. and Spitteler, P.H.J., 1996. Experimental observations on the pressure-dependent polymer melt rheology of linear low density polyethylene, using a multi-pass rheometer, *Rheologica Acta*, **35**, 202.

[63] Binding, D.M., Couch, M.A. and Walters, K., 1998. The pressure dependence of the shear and elongational properties of polymer melts *J. Non-Newtonian Fluid Mech.,* **79**,137-155.

[64] Sedlacek, T., Zatloukal, M. Filip, P. and friends., 2004. On the Effect of Pressure on the Shear and Elongational Viscosities of Polymer Melts *Society of Plastics Engineers,* **44**,1328-1337.

[65] **Sombatsompop, N. and Dangtungee, R.,** 2001. Effect of die design on flow visualization and die swell of NR in a capillary rheometer, *Journal of Materials Science Letters,* **20**, 1405-1408.

[66] **Sombatsompop, N. and Intawong, T.,** 2005. A comparative study on extrudate swell ratio of polystyrene in a capillary rheometer and a single screw extruder, *Polymer Testing*, **24**, 948–952

[67] **Liang, J.Z. and Ness, J.N.,** 1998. The Melt Die-Swell Behaviour During Capillary Extrusion of LDPE/PP Blends, *Polymer Testing,* **17**, 179-189.

[68] **Kelly, A.L., Coates, P.D., Dobbie, T.W., and Fleming, D.J.,** 1997. On line rheometry: shear and extensional flows, *Plastics, Rubber and Composites Processing and Applications,* **25**, 313.

[69] **ASTM D 3835 -96,** Standard test method for determination of properties of polymeric materials by means of a capillary rheometer, USA.

[70] www.malvern.co.uk/rosand ,2007.

[71] www.celsum.com/eta2100.htm ,2007.

[72] www.goettfert.com ,2007.

[73] www.rheologysolutions.com/rheocaps_techs.html ,2007.

[74] **Rides, M. and Allen. C.,** 2006. Slip flow measurement by capillary extrusion rheometry, Allen Division of Engineering and Process Control National Physical Laboratory, Teddington.

[75] **Robert L. Mott,** 2004. Machine Elements in Mechanical Design, Pearson Education, USA

[76] http://www.malvern.co.uk/LabEng/products/bohlin/rh2000/capillary_rheometers_faq.htm ,2007.

[77] www.rheologysolutions.com/rheocaps_techs.html ,2007.

[78] www.ceast.com ,2007.

[79] http://www.dynisco.com/products/pt/datasheets/7000_3.pdf ,2007.

[80] Mitsoulis E., Hatzikiriakos S., Christodoulou K., and Vlassopoulos D., 1998**.** Sensitivity analysis of the Bagley correction to shear and extensional rheology, Rheol Acta 37:438–448.

CV

İsminur Gökgöz was born in Iskenderun in 1978. She graduated from Iskenderun High School in 1995 and Physics division of Yıldız Technical University in 2000. Then she took foreign language training, English, in ITUSEM. In 2004, she began to Polymer Science and Technology master program in Istanbul Technical University. Until January 2008, she has working as an trainee in Dizayn Group Company and prepared her thesis in RTD department. She is still working in this department.